![UiT The Arctic University of Norway]

Faculty of Engineering Science and Technology

Review and Application of Optimal Sensor Placement Method on Herøysund Bridge

Macdonald Nwamma

Master's thesis in Engineering Design END 3900 May 2023

Abstract

The study attempts to find the best sensor configuration for modal identification on the Herøysund Bridge. The objective is to increase the amount of data obtained from structural testing while reducing the number of sensors needed thereby reducing the cost of the sensor system. Four frequently used optimal sensor placement (OSP) methods, including the modal kinetic energy (MKE) method, the effective independent (EFI) method, minimum modal assurance criterion (MinMAC) method, and the information entropy (IE) method is explored and discussed. The EFI method is selected and applied on a beam model of the bridge, both with and without post-tension. An algorithm is written on MatLAB using as input data the modal analysis results of the bridge obtained from ANSYS. A modified EFI method known as the effective independence driving point residue (EFI-DPR) method is also considered, and its final sensor locations set compared to those obtained from the EFI method. Both methods are validated by the condition number, trace, and determinant of the Fisher information matrix (FIM). Additionally, an interface is established to link ANSYS to MATLAB for the purpose of performing the sensor placement methods. The outcome of the Herøysund Bridge case study shows that the EFI-DPR method is more effective than the EFI method because it maximizes its performance criterion.

Acknowledgment

Macdonald Elochukwu Nwamma

Narvik, May 2023.

Contents

List of Tables

List of Figures

List of Symbols

A	Matrix
A^T	Transposed of A
A^{-1}	Inverse of A
$A \otimes B$	Term-by-term multiplication
E(X)	Expected value of a variable
λ	Eigenvector
ψ	Eigenvalue
Σ	Sum
σ	Singular value
$\hat{q}$	Target states
ψ_o^2	Gaussian white noise variance
ω	Target mode frequency
θ_o	Optimal value of parameter set

List of Abbreviations

DOF   Degrees of freedom
DPR   Driving point residue.
EFI   Effective independence
EOT   Energy optimization technique
FE   Finite element
FIM   Fisher information matrix
IE   Information entropy
MAC   Modal assurance criterion
CM   Condition monitoring
MinMAC   Minimum modal assurance criterion
ED   Effective independence distribution vector
FSSP   Forward sequential sensor placement
WPT   With post-tension
WNPT   With no post-tension
MKE   Modal kinetic energy

1. Introduction

Structural health monitoring (SHM) has become a crucial area in the field of infrastructure development, particularly for high-rise buildings, bridges, and other complex structures. SHM techniques provide valuable information about the health of structures to ensure they are safe, reliable, and cost-effective. The performance of these techniques, such as vibration and strain monitoring, heavily relies on the optimal placement of sensors on structures. The placement of sensors is a challenging task, and an effective method of OSP can significantly reduce the number of sensors required, thereby reducing SHM costs. OSP methods have, therefore, become a vital area of research in the field of SHM, attracting the attention of researchers worldwide.

Various OSP methods have been developed, each with its own advantages and limitations. Some of the most commonly used OSP methods include EFI, IE, and MKE. EFI is a method that seeks to maximize the spatial diversity of sensors, while IE seeks to maximize the information content of the sensor data. MKE, on the other hand, seeks to place sensors in areas where the modal kinetic energy is expected to be high, indicating a high structural response.

This thesis aims to provide a comprehensive review of existing OSP methods, including EFI, IE, and MKE methods, and finally present practical applications of one of these OSP methods to real-life scenarios in the field of infrastructure development.

1.1. Purpose of study

The thesis shall review and apply an optimal sensor method of the Herøysund Bridge to obtain the best sensor network from an initial much larger set of sensor locations for accurate identification of target modes partitions and cost reduction.

1.2. Limitations

The thesis will focus on reviewing commonly used OSP methods and the application of the EFI methods on beam models of the Herøysund Bridge. A comparison between sensor configuration obtained from the EFI method and the EFI-DPR method will also be performed.

1.3. Outcome

The documentation shall give an understanding of the four commonly used optimal sensor placement methods with more focus on the EFI method which has been selected for this study based on a recommendation by one of my supervisors.

2. Literature study

2.1. Damage identification and evaluation

Over time, humans have consistently created and maintained innovation by developing numerous systems and engineering structures that promote functional environments. Unfortunately, such infrastructures are often susceptible to severe damage due to several factors, including high loads, environmental factors, structure degradation, and material characteristics, leading to the emergence of structural assessment methods [1]. Damage can be described as modifications to a system's geometric and material characteristics, including boundary conditions and system connectivity, negatively affecting the system's current or future performance [2].

The monitoring and measurement of damage are vital in various multidisciplinary areas, including SHM, condition monitoring (CM), non-destructive evaluation (NDE), and statistical process control (SPC) [3]. SHM is utilized for structures such as buildings and aircraft, utilizing sensor networks to track the structure's behavior online. On the other hand, CM relies on vibration and accelerometer sensors to track changes in the behavior of rotating and reciprocating machinery. NDE primarily employs offline techniques such as ultrasound, thermography, and shearography to characterize and assess the severity of damage. However, SPC, which is process-based rather than structure-based, utilizes a variety of sensors to track changes in the process [3].

2.2. Structural health monitoring

Structural Health Monitoring is a process of monitoring and assessing the structural condition of buildings, bridges, and other infrastructure over time to identify defects, damages, or performance degradation. This is achieved through the periodic measurement of the mechanical system or structure and the extraction of damage-sensitive features from these measurements, followed by statistical analysis to establish the present system's health [4]. According to Scuro *et al* [5], SHM systems are designed to monitor aspects such as humidity, temperature, accelerations, tensile stress, compressive stress, and degradation of building materials. The techniques employed are non-invasive and necessitate the installation of sensors at specific locations defined by experts. The data collected by the sensors is then integrated with mathematical models to determine the safety of the structure [5].

An SHM system is typically intended to achieve the following goals:[6] confirm the viability of modifications made to an existing structure with the aim of enhancing design specifications; detect external loads and responses, and forecast potential deterioration to evaluate the safety of a structure; provide evidence to facilitate the planning of structure inspection, rehabilitation, maintenance, and repair, and evaluate the effectiveness of maintenance, retrofit, and repair works; and gather a wealth of in-situ data for further exploration of

structural engineering, including earthquake-resistant designs, innovative structural types, and the application of smart materials. In otherwords, SHM aims to provide early warnings of potential structural problems and prevent catastrophic failures, improve safety, reduce maintenance costs, and extend the structure's life.

2.3. Optimal sensor placement

The monitoring of mechanical and civil structures requires the use of sensors that needs to be placed at designated locations to accurately measure their dynamic parameters; hence, the reason OSP is important. OSP involves defining the minimum number of sensors and their arrangement to decrease the invasiveness of the monitoring system, lower energy consumption and cost, minimize the amount of collected data while retaining useful information, optimize the monitoring system's longevity, network coverage, and durability [7].

The problem of sensor placement is divided into three aspects [8]. Firstly, determining the minimum number of sensors required for dynamic testing. Secondly, deciding where to place those sensors, and finally, evaluating the effectiveness of different placement methods. The minimum number of sensors required is determined by the observability of the structure, but practical considerations often result in a larger number of sensors being used.

The second aspect is the most important and depends on the third aspect, which involves developing a suitable performance measure and selecting an appropriate optimization method. The third aspect includes various methods for assessing the performance of chosen sensor sets. Ultimately, the number of sensors required can only be determined after the second and third aspects have been addressed. Some of the criteria for OSP will be discussed in the following sections. However, a traditional criterion utilized by experts for OSP is simply based on engineering experience or intuition [8].

Kammer [9] proposed the EFI criterion, which ranks candidate sensor locations according to their contribution to the linear independence of the target modes. This process developed by Kammer, is an iterative one, and ensures that locations that do not offer significant contributions are removed. The criterion was applied to a finite element (FE) model of an elastic beam used as a simple representation of a large space structure (LSS). In another paper, Kammer [10] considered the effect of sensor noise at the candidate sensor location. A noise model was developed, which, when introduced to the EFI criterion, resulted in a higher ranking of sensor locations with low noise levels and suppression of those with high noise levels.

In a different paper, Sunca *et al.* [11] implemented the EFI criterion on a laminated composite cantilever beam and two steel cantilever beams with hollow circular and box cross-sections. Friswell and Castro-Triguero [12] also applied this method on a cantilever beam and investigated the relationship that exists between the method, and the mode shapes linear independence. A modification of the EFI criterion, the EFI-DPR, was

introduced by Li *et al.* [13] and focused on a vector called the Driving Point Residue (DPR) which was multiplied by the EFI criterion. The EFI-DPR sensor placement criterion, which was applied on the Xinghai Bay Bridge, ensures sensor locations with low signal-to-noise ratio are not selected during the utilization of the EFI criterion. Similarly, the EFI-DPR criterion was applied to the Nottingham suspension bridge by Meo and Zumpano [14].

According to the MKE, the optimal placement of sensors is achieved by identifying the locations on the structure where the modes of interest have maximum kinetic energy. This is based on the assumption that sensors placed at these locations will provide the highest level of observability for those modes. Leyder *et al.* [15] used the modal kinetic method for the implementation of OSP on a timber frame structure. Meo and Zumpano [14] employed the MKE method for sensor placement on the Nottingham Bridge. Also, the method is applied on an I-40 bridge located in Albuquerque, New Mexico [16]. Kammer [9] also applied this method for the identification and ultimate test-analysis correlation of bending modes of 15 main truss.

Li *et al.* [17] applied the minMAC for the purpose of determining the OSP in the health and monitoring system of the Xinghai Bridge in China. The minMAC method was also implemented on a footbridge on Princeton University campus by Lizana *et al.* [18] for modal identification of the bridge, while Leyder *et al.* [15] also implemented the minMAC method in determining the optimal sensor configuration for dynamic structural identification of a post-tensioned timber frame structure.

A statistical methodology was presented in this paper by Papadimitriou *et al.* [19], which employed the information entropy criterion in optimal sensor location for a structure with the aim of extracting the most information about the model parameters from the measured data. Meanwhile, this study by Zhang *et al.* [20] developed an optimal sensor strategy using the information entropy criterion to ensure reference and roving sensors are optimized simultaneously.

2.4. Optimal sensor placement criteria

The criteria used to determine the suitability of sensor configuration vary depending on the specific application. In this section, we will briefly discuss several influential criteria that have impacted sensor placement theory over time. See full detailed information in reference.

2.41. Modal assurance criterion

One criterion is MAC, which requires that the measured mode shapes be as linearly independent as possible in order to distinguish the identified modes [21]. This is important when validating or updating finite element models. When selecting measuring points, it should be ensured that the solid angle between the measured modal vectors is relatively

large in order to maintain the original characteristics of the structure [21]. The MAC is a scalar constant that relates the causal relationship between two modal vectors. Typically, the criterion is applicable to the comparison of experimental mode shape vectors to those obtained numerically. However, mode shape vectors from either same FE model or those from two FE models can also be compared [22].

$$MAC_{ij} = \frac{(\Phi_i^T \Phi_j)^2}{(\Phi_i^T \Phi_i)(\Phi_i^T \Phi_j)}, \tag{2.0}$$

where $\boldsymbol{\Phi_i}$ and $\boldsymbol{\Phi_j}$ are the ith and jth column vectors in matrix $\boldsymbol{\Phi}$, respectively, and subscript T represents the transpose of the vector [22].

The MAC values range from 0 to 1, where a value of 1 indicates a strong correlation between the two modes being compared, and a value of 0 shows that there is little or no correlation between the modes [23].

MAC values can also be displayed in a matrix format where modal vectors are seen as highly correlated when the off-diagonal elements are close to 1 and not correlated when off diagonal elements are approaching 0. An optimal set of modal vectors will have a diagonal MAC matrix, and the size of the off-diagonal elements will indicate the quality of the results [22].

2.42. Fisher information matrix

Another criterion is the FIM which can be obtained from the minimization of the covariance matrix of the estimate error for an efficient unbiased estimator from the perspective of statistics. The FIM criterion is given as follows [22]:

$$FIM = \Phi^T \Phi, \tag{2.11}$$

where Φ is an *[n x n]* mode shape matrix (or *[m x m]* matrix if m target modes are considered), and *T* represents a transpose of the mode shape matrix.

The FIM criterion aims to unselect candidate sensor positions such that the FIM is maximized. Three variants of the FIM are used in practice, including the determinant, the trace, and the minimum singular value of the FIM, which are either maximized to increase the information or decrease the uncertainties associated with the estimates [22].

2.43. Measured energy per mode

Measured energy per mode is a third criterion that considers the distribution of kinetic energy in a structure's modes. The degree of freedom (DOF) selected to measure the modes should capture a large portion of the total kinetic energy of the structure, and the energy contained in the measured DOFs for each mode should be a significant portion of that mode [22]. This criterion Yi and Li believes helps to select sensor positions with

possible large amplitudes and to increase the signal-to-noise ratio, which is crucial in noisy and harsh environments.[22]

2.44. Information entropy

The IE measures the amount of uncertainty present in the parameters of a system. A low IE indicates minimal uncertainty in the system parameters and a high level of useful information in the collected data [24]. Therefore, when selecting a sensor configuration, the goal should be to minimize the IE. The IE for a specific sensor configuration *(L)* can be written as (see [24]):

$$IE(L, \theta_o) = \frac{1}{2} N_\theta In(2\pi) - \frac{1}{2} In[\det\{Q(L, \theta_o)\}], \qquad (2.12)$$

where, θ_o represents the optimal value of the parameter set θ of length N_θ (number of parameters) that minimizes the IE and $Q(L, \theta_o)$ is the *[N_θ x N_θ]* FIM. For modal identification, the focus is on the modal coordinates, which are the parameters of interest. In this case, the parameter set θ becomes a *[m x l]* vector for *m* target modes and FIM becomes a *[m x m]* matrix [24].

3. Sensor placement methods

There exist different methods or criteria used for optimal sensor placement. In this chapter, we shall discuss four different methods: the EFI method, the EFI – DPR method, the MKE method, and the minMAC method. Each of these methods' fundamental concepts and theories is thoroughly discussed.

3.1. Effective independence method

The EFI method is indeed a popular technique that has been shown to be effective and efficient for sensor placement in various applications, including modal testing, model updating, and damage detection for sensor placement in structural engineering applications [25]. The aim of the EFI method is to select measurement positions that make the mode shapes of interest called target modes as linearly independent as possible while containing sufficient information about the target modal responses in the measurements [25]. The EFI method is based on a sequential sensor placement approach, where sensors are added to a structure one at a time, and at each iteration, the sensor with the lowest value in the effective independence distribution vector (ED) is removed until the desired number of sensors is reached [25]. The output sensor response can be defined using equation (3.0)

$$u_s = \Phi_s q, \tag{3.0}$$

where Φ_s is the matrix of FEM target modes divided according to their corresponding sensor locations, and q is the modal coordinate vector [25].

By resolving Equation (3.0), the sensors can be sampled, and an estimate for the target states $\hat{q}$ can be calculated.

$$\hat{q} = [\Phi_s^T \Phi_s]^{-1} \Phi_s^T u_s, \tag{3.1}$$

where u_s and Φ_s have been defined in equation (3.0), further, T is the transpose of the mode shape matrix, and is the location in the candidate sensor set.

The best estimate of the target states can be obtained when the covariance matrix of the estimate error is at its minimum. Therefore, the output equation (3.1) is modified (see [25])

$$u_s = H(q) + N = \Phi_s q + N, \tag{3.2}$$

where $H(q)$ represents the process measurement and vector N is the stationary Gaussian white noise variance Ψ_0^2. For an efficient unbiased estimator, the covariance matrix of the estimate error given by

$$P = E[(q - \hat{q}_F)(q - \hat{q}_F)^T] = [\Phi_s^T R^{-1} \Phi_s]^{-1} = Q^{-1}, \tag{3.3}$$

in which Q is the FIM. But the unbiased estimator of the target state response, which is produced by the Fisher model estimator, W_F, can be written as (see [26])

$$\hat{q}_F = W_F u_s = [\Phi_s^T R^{-1} \Phi_s]^{-1} \Phi_s^T R^{-1} u_s \tag{3.4}$$

The sensor noise N is uncorrelated and possesses identical statistical properties to, each sensor. Therefore, the FIM can be expressed as

$$Q = \frac{1}{\sigma^2} \Phi_s^T \Phi_s = \frac{1}{\sigma^2} A_o \tag{3.5}$$

Since the covariance intensity matrix R is

$$R = \sigma^2 I, \tag{3.6}$$

where σ^2 is the sensor noise variance and I is an identity matrix which means all the off-diagonal elements in R are zero [26].

According to Kammer, [9] E can be calculated as

$$E = \Phi_s \psi \lambda^{-1} \psi^T \Phi^T = \Phi_s A_o^{-1} \Phi_s^T, \tag{3.7}$$

where ψ and λ are the eigenvector and eigenvalue matrix of Q, respectively.

The Matrix E is a projector that is orthogonal and is used to identify the column space of the target modes [9]. Kammer also believes the trace and rank are equivalent, which is significant because the diagonal elements of matrix E represent the contribution of each sensor location to the rank. As the rank is associated with the number of linearly independent target modes, the diagonal elements of matrix E indicate their contribution to the independence of the target modes [9]. The trace is also linked to the diagonal of the matrix as it represents the sum of the diagonal elements of the matrix. The vector containing these diagonal elements is called the effective independence distribution vector (ED) and terms in the ED vector are utilized to rank the sensor locations and undergo an iterative elimination process where the smallest magnitude term is removed until the required number of sensors is achieved [10].

3.2. Effective Independence - driving point residue method

The EFI-DPR technique was developed to address the drawback experienced when the EFI method is implemented for optimal sensor placement. It was discovered that sensors that possess low energy content may be selected when the EFI method is used, and this could lead to loss of information [27]. Thus, the EFI-DPR technique solves this problem by multiplying the candidate sensor contribution of the EFI method with the corresponding DPR coefficient:

$$DPR_i = \sum_{j=1}^{N} \frac{\phi_{ij}^2}{\omega_j}, \tag{3.8}$$

which changes the EID vector expression (see [28]):

$$E_{Di} = [\phi\psi]^2 \lambda^{-1}\{1\}_i DPR_i, \tag{3.9}$$

where ϕ_{ij} is the *ith* nodal displacement of the *jth* mode shape, ω_j is the *jth* target mode frequency, and $\{1\}_i$ is the sum of all coefficients belonging to row *i*. The DPR functions essentially as an ED vector weighting factor. By concentrating sensor locations in areas with high energy content, this approach deploys sensors that are roughly regularly distributed and symmetrical [14].

3.2. Modal kinetic energy method

The MKE method is another method for optimal sensor placement, and its approach is like an EFI method but with a different objective. The MKE technique aims to position sensors in locations where the kinetic energy is maximal. Furthermore, optimizing sensor placement based on the MKE matrix yields a superior signal-to-noise ratio for mode shape detection [29].

One crucial factor for this method is that the mass and stiffness matrices should be reduced to capture only relevant DOF from the FE model required for computation. This is important because it eliminates excess time spent on computation and further improves processing efficiency. Therefore, the matrices can be reduced through the Guyan reduction method using the formulas (see [29])

$$K_R = T'KT, \tag{3.10}$$

$$M_R = T'MT, \tag{3.11}$$

where K_R and M_R are the reduced stiffness and mass matrices respectively, meanwhile; *T* is the transformation matrix which is given as

$$T = \begin{bmatrix} I \\ -K_{sm}^{-1} \, K_{mm}' \end{bmatrix}, \tag{3.12}$$

where *I* is an identity matrix, and its size is determined by the master degree of freedom, *m,* which is the DOF that the user is interested in. The unchosen DOFs following the selection of the master DOFs are categorized as the slave *s* DOF [29].

Heo *et al.* [27] proposed the kinetic energy optimization technique (EOT), which describes the distribution of kinetic energy in the system as

$$KE = \Phi^T M \Phi, \tag{3.13}$$

where Φ is the measured mode shape matrix, and *M*, in this case, is the mass matrix, but for this thesis, would be replaced with the reduced mass matrix, M_R. The EOT ensures the kinetic energy is maximized while maintaining the spatial independence of the mode shapes. However, a new kinetic energy matrix will be obtained after the decomposition of the mass matrix into upper *(U)* and lower *(L)* triangular Cholesky factors that are (see [27]):

$$M = LU \quad and \quad \Psi = U\Phi \tag{3.14}$$

Therefore,

$$KE = \Psi^T \Psi \tag{3.14}$$

The similarity between the effective independence and the modal kinetic methods becomes evident at this point, where the new KE matrix is obtained. This matrix holds the same information as the fisher information matrix *Q* obtained from the EFI method [14]. The EOT vector is then developed using the fractional contribution of each sensor location to the modal kinetic energy matrix, which is given by the equation [27]:

$$EOT = \sum_{i=1\ldots k} \left[\Psi \psi \Lambda^{-\frac{1}{2}} \right]^2, \tag{3.16}$$

where Λ is the eigenvalue and ψ is the eigenvector of the kinetic energy matrix, the square represents a term-by-term square of the enclosed matrix, and dimension k corresponds to the number of mode shapes. The sensor location with the lowest value is removed from the EOT vector, and its corresponding row is eliminated from the kinetic energy matrix [14]. This process is iterative and should be repeated until the desired number of sensor locations is obtained. Nevertheless, after every sensor elimination, the newly formed matrix is examined for rank deficiency. If removing the sensor location results in rank deficiency, it means that the location should not be removed [14].

3.3. Minimum modal assurance criterion

The MinMAC method is an iterative method developed by Carne and Dohrmann [16], which is based on the forward sequential sensor placement (FSSP) algorithm and the MAC for determining the number and location of sensors.

It is important to establish the normal mode indicator function which is required for the determination of the combination of exciting locations and directions that can excite all the target modes. Carne and Dohrmann also believes the normal mode indicator function for a chosen set of sensors is computed by using intuition to select several locations and directions in combination with mode shape knowledge. A mode indication function values between 0 and 1 indicates that a mode is excited well and can be easily extracted from the measured frequency response functions (FRFs) for that excitation [16].

Some correspondence needs to be developed between the analytical mode shapes and those obtained from tests or experiments without assumptions that both would maintain similar numerical order. To do this, the MAC is used for the evaluation of the square of the cosine between the shape vectors as shown below in (3.17) thereby ensuring the shape vectors are distinguishable.

$$MAC_{ij} = \frac{(\Phi_i^T \Phi_j)^2}{(\Phi_i^T \Phi_j)(\Phi_i^T \Phi_j)},$$

(3.17)

where $\boldsymbol{\Phi_i}$ and $\boldsymbol{\Phi_j}$ are the mode shape vectors for the *ith* and *jth* modes. It is crucial to obtain a MAC matrix whose off-diagonal elements are relatively small in order to easily distinguish shape vectors which can be achieved through the addition of sensors one at a time to a small set of locations selected based on intuition known as the intuition set. Therefore, a method is needed to evaluate the effect of the sensors added to the MAC matrix [21].

Assuming a *(n x m)* mode shape matrix for the intuition set Φ and *an ($\hat{n} \times m$)* matrix containing the remaining DOF $\hat{\Phi}$ where *n* represents the number of DOF in the existing sensor set and $\hat{n}$ is the number of remaining DOF which can still be selected, and *m* the number of modes, the MAC value between modes *i* and *j* can then be expressed as (see [21]):

$$MAC_{ij} = \frac{a_{ij}a_{ij}}{a_{ij}a_{ij}},$$

(3.18)

where a_{ij} are the elements of A = $\Phi^T\Phi$. When row k of $\hat{\Phi}$ is added to Φ, the MAC value between modes *i* and *j* becomes

$$\left(MAC_{ij}\right)_k = \frac{\left(a_{ij} + \hat{\Phi}_{ki} \hat{\Phi}_{kj}\right)\left(a_{ij} + \hat{\Phi}_{ki} \hat{\Phi}_{kj}\right)}{\left(a_{ii} + \hat{\Phi}_{ki} \hat{\Phi}_{ki}\right)\left(a_{jj} + \hat{\Phi}_{kj} \hat{\Phi}_{kj}\right)}$$

(3.19)

The matrices $\hat{\Phi}, \Phi,$ and A are updated each time a sensor is added to the existing set, and then the candidate sensor evaluation process continues using one of the following methods below [21]:

Method 1: The sensor leading to the smallest maximum above diagonal MAC value in the

entire matrix is chosen. This method requires that equation (3.19) is used $m(m\text{-}1)\,\hat{n}/2$ times for each sensor added.

Method 2: method 2 is similar to method 1 but introduces a more efficient approach when there are numerous modes (or sensors) to consider. Instead of tracking all above-diagonal MAC values, only p values are considered. Initially, p is set to 1. The method involves finding the sensor that minimizes the maximum of these p tracked MAC values. By iteratively adding sensors and updating the maximum value, the process continues until a suitable sensor is found. This approach reduces computation time when dealing with a large number of potential sensors.

4. Case Study: Herøysund Bridge

4.1. Description

Herøysund Bridge is a 154.5m long concrete bridge in Herøy municipality, Nordland County, connecting south and north Herøy, and assumed to be built on a rock. It has a main span of 60m and is divided into seven axes comprising five pillars and two land vessels [30].

Figure 1: Overview of the Herøysund Bridge

The girder bridge was built in 1966 and has a single lane with narrow sidewalks on both sides as shown in figure 1. It also has a bridge slab and two beams beneath bearing its load. A Pressure plate was cast towards the main pillars on axis 4 and 5, while axis 3 to axis 6 has been span–reinforced [30]. The four post-stressed cables on each of the two girders on the north and south sides are each anchored at axis 6 in the west and axis 3 in the east [31]. About 15 meters on either side of the bridge's Centre are where each cable has one of its two joints. The girders are 400 mm thick and 1000 mm high between the bottom and underside of the bridge deck [31].

According to the report [31], The Herøysund Bridge has been subjected to several tests and maintenance checks to understand its current state. It was discovered that parts of the pre-stressing reinforcement are corroded, and the beams placed longitudinally lacks any form of slack reinforcement. Cracks ranging from 0.5-0.9mm appeared on different parts of the beam in the middle of the main span of the bridge and Grouts were also found to be missing in the tendon ducts and some of the cables had wire breakage [31] As a result, it has become necessary to monitor the health of the bridge by using sensors installed at designated locations, at low costs, which produce relevant data that would influence maintenance decision and possibly extend the lifespan of the structure while a replacement is being constructed. Therefore, the main aim of this project is to obtain an optimal sensor

configuration using the EFI. The results obtained would also be compared to those obtained from the EFI-DPR method.
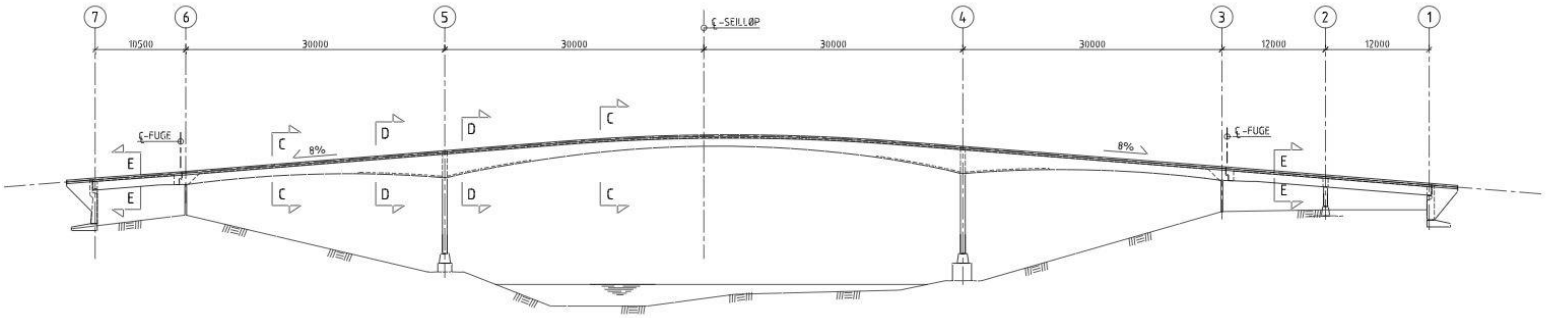

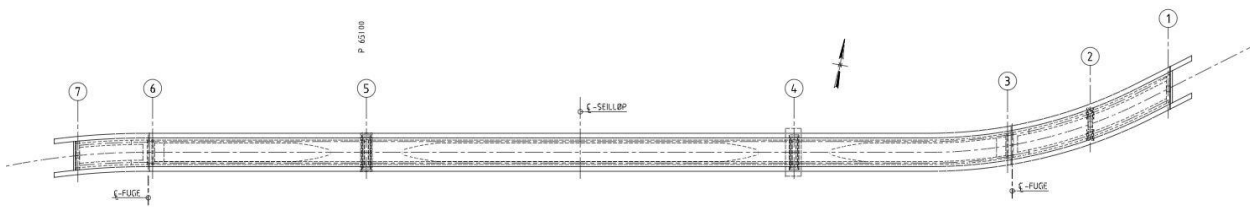Figure 2: Side view of Herøysund Bridge[30]
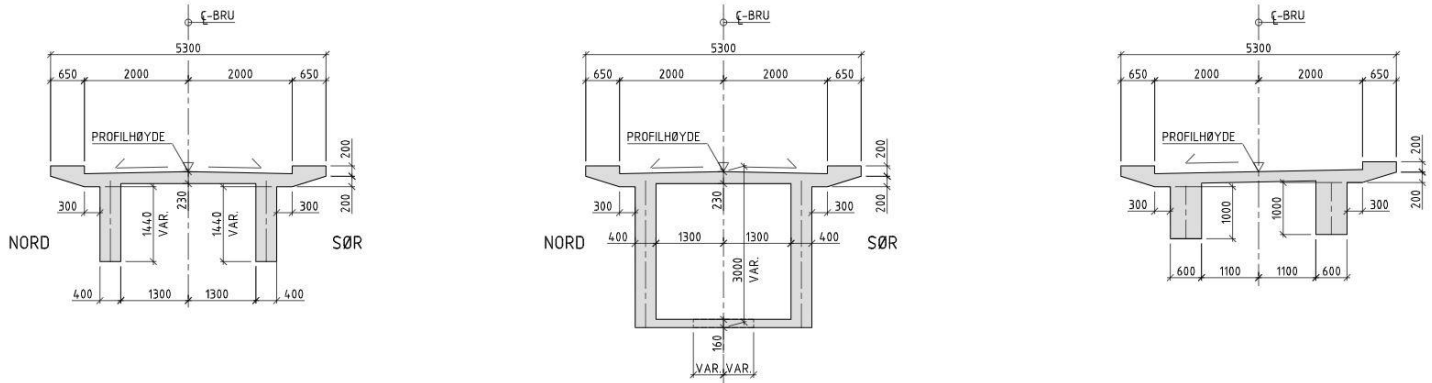

Figure 3: Plan view of Herøysund Bridge[30]

Figure 4: Cross-section of Herøysund Bridge[30]

4.2. Finite Element Model

Three-dimensional finite element (FE) models of the Herøysund Bridge were designed to provide input data for applying both the EFI and the EFI-DPR methods in order to find

optimal sensor locations. The models are beam-type models designed by Patrick [32] on ANSYS Spaceclaim and then exported to ANSYS Workbench for further analysis.

4.2.1. Beam Model

The beam model is in two forms: one with post-tensions (WPT) and the other with no post-tensions (WNPT). Post-tensioning is a technique used in bridges and other structures to strengthen and reinforce concrete. In this technique, high-strength steel strands or tendons are placed in the concrete and stressed to a predetermined level of tension using hydraulic jacks, and then anchored to the concrete with steel plates and wedges. This compresses the concrete, resulting in increased strength and stiffness of the structure. The main function of post-tensioning in bridges is to increase their load-carrying capacity and reduce the effects of cracking, deflection, and other types of deformation thereby ensuring higher resistant to damage and ultimately reducing maintenance costs over its lifespan.
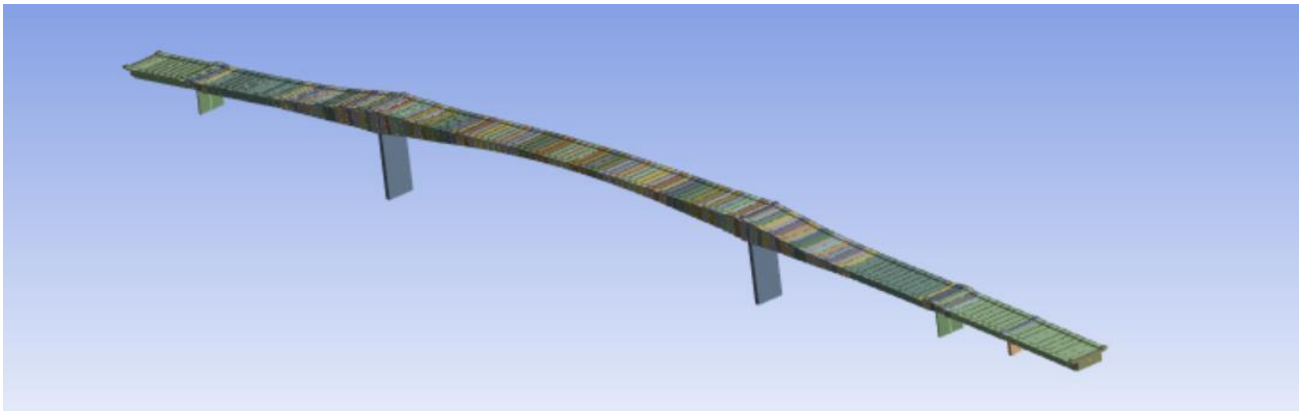
Figure 5: Finite element model of Herøysund Bridge [32]

The finite element models are designed such that the bridge's width is across the Z axis, its span along the X axis, and the Y axis orthogonal to the XZ plane. Both models WPT and WNPT have an element size of 100mm, which generated a total number of 1834 elements and 3672 nodes. ANSYS mechanical was used to perform the modal analysis where 20 mode shapes were obtained and analyzed. The dynamic parameters for six target modes obtained from each of the models were extracted to MATLAB and used to apply the OSP method. The natural frequencies and mode shapes of the Herøysund bridge finite element model for both cases can be seen in the table 1 and figure 6 below:

Table 1: Frequencies of model with post-tension and model with no post-tension

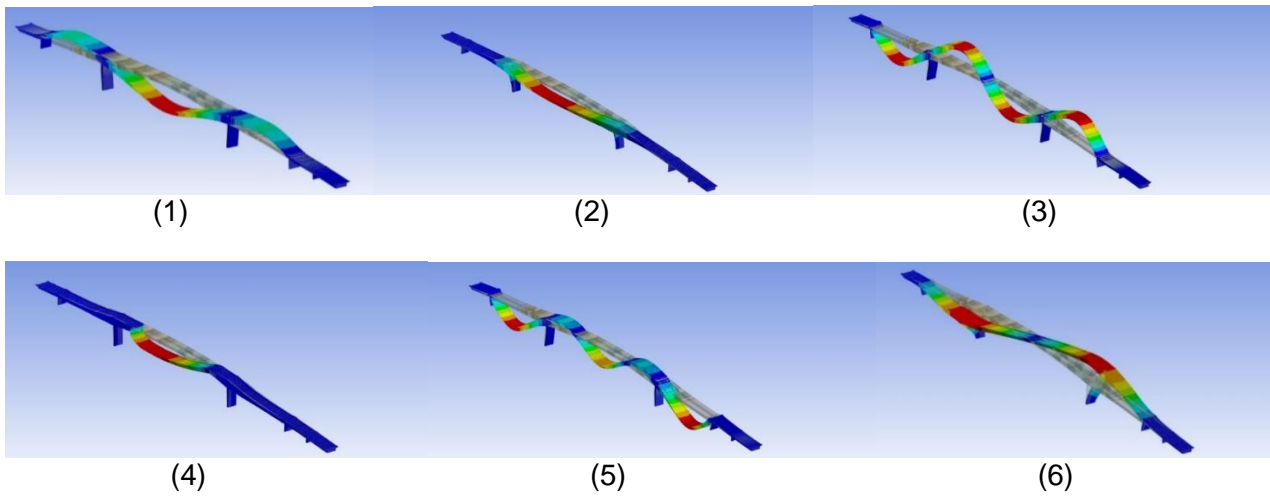| Mode	Frequency [Hz]	
	WPT	WNPT
1	1.4407	1.4413
2	2.2387	2.2388
3	2.3951	2.3961
4	2.9588	2.9593
5	3.5732	3.574
6	4.1455	4.1456

(1)

(2)

(3)

(4)

(5)

(6)

Figure 6: Target mode shapes of the Herøysund Bridge beam model [32]

5. Results

5.1. Application of the Effective Independence method

Mode shapes obtained from the Bridge model are used to carry out the EFI approach. A total number of 20 modes were obtained for both models WPT and WNPT. However, only the first 6 modes in both models were considered as target modes for the application of the EFI methods. These target modes are then imported from ANSYS into MATLAB, where sequential sensor placement is used to minimize the number of sensor positions from 5514 to 10. The lowest ED value in each iteration is eliminated together with its corresponding row in the mode shape matrix and continues up until the necessary number of sensors is obtained.

The final sensor locations can be visualized from the MATLAB plot in figure 7 below. The plot was obtained after carrying out the EFI method on the Herøysund Bridge model WPT. It can be observed that some locations have two sensors in both Y and Z directions and almost have good spatial distribution.

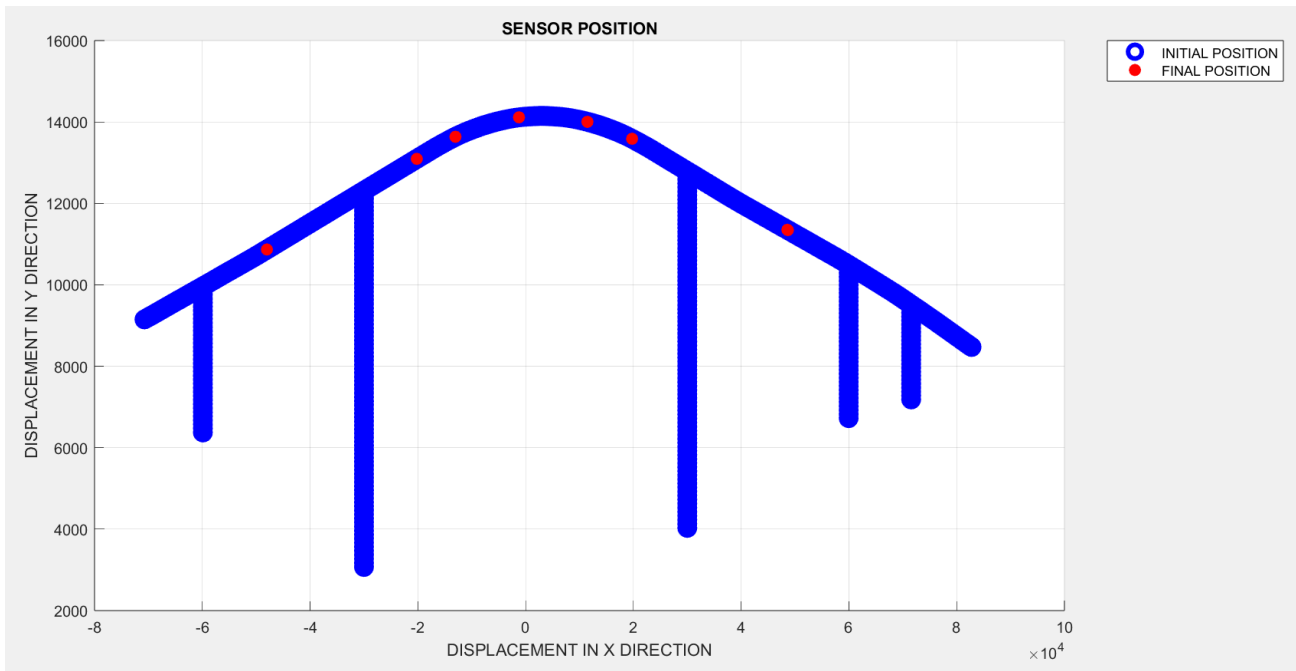Figure 7: Ten final sensor location for model WPT using EFI method

However, the result from the plot in figure 8 shows that the final sensor locations after the application of the EFI-DPR method have a symmetric and quasi-uniformly spaced sensor configuration.
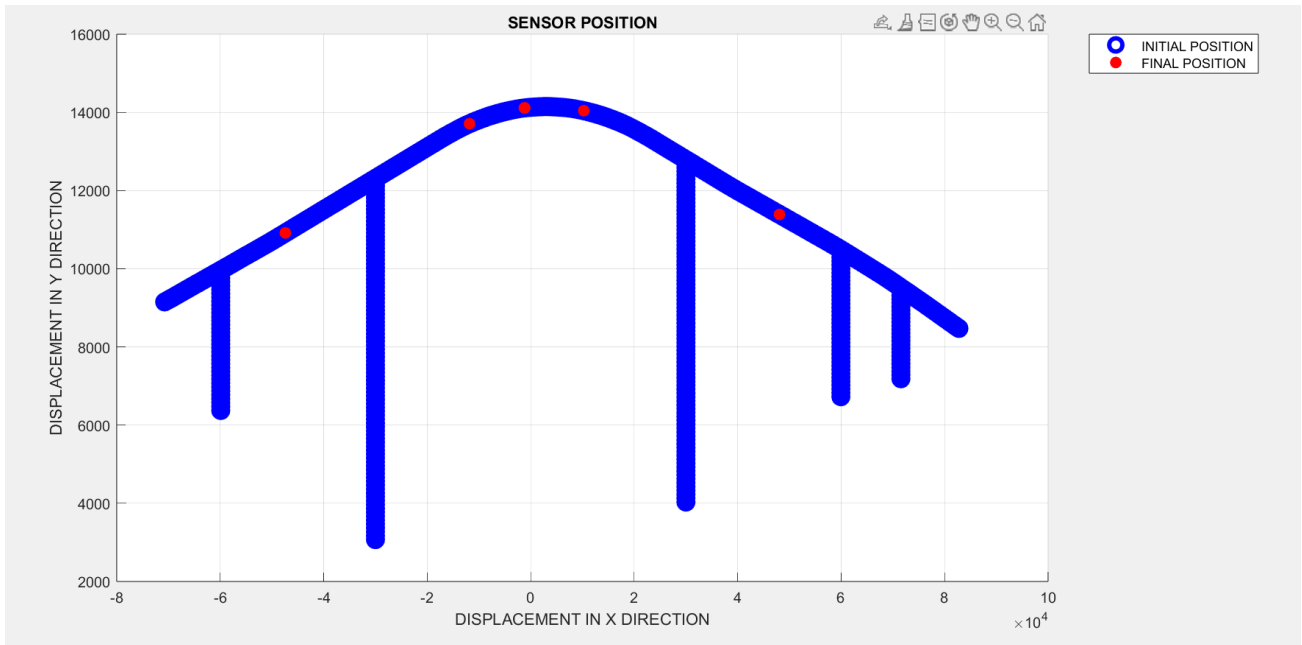
Figure 8: Ten sensor locations for model WPT using EFI-DPR method
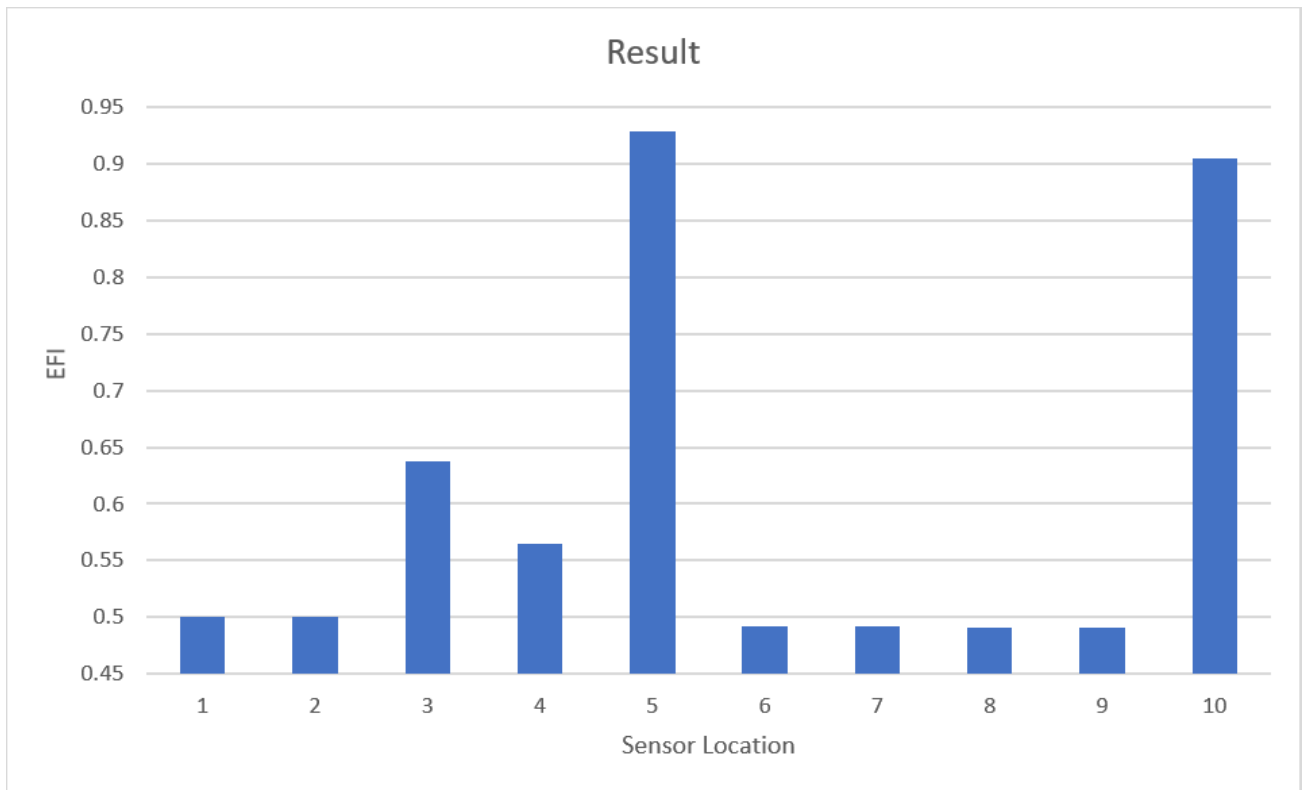
Figure 9: Bar plot of ED values for ten sensor locations for beam model WPT
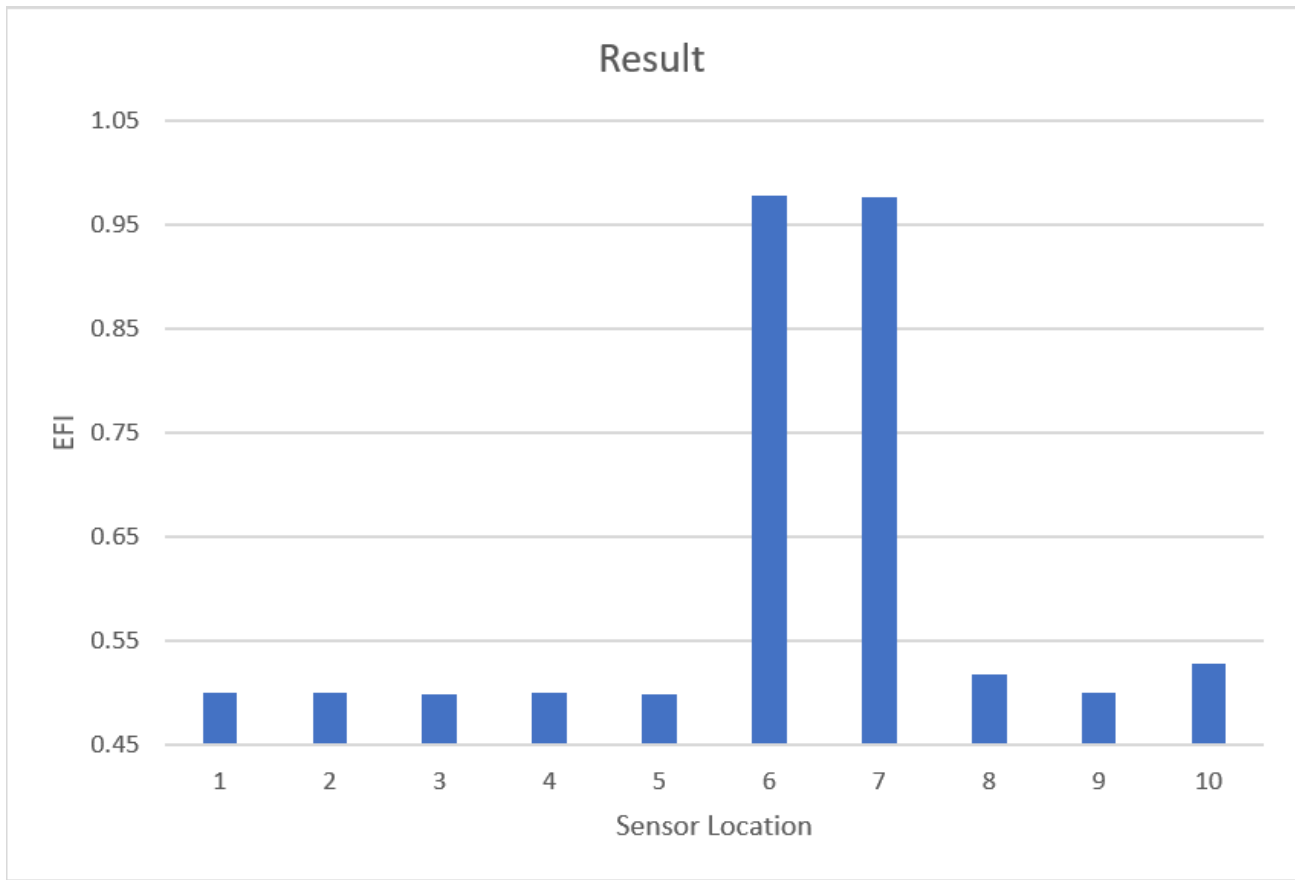
Figure 10: Bar plot of ED values for ten sensor locations for beam model WNPT

The values in the effective independence distribution vector (ED) for the final ten sensor locations are displayed in figure 9 and figure 10 above for both model with PT and those without PT. The final sensor positions are represented in the X-axis and the EFI ED values in the Y-axis. Due to the close proximity of some of the values in the ED vector, the vertical scale does not begin at zero in order to highlight the difference. The ED values are also given in table 3.1 with their corresponding final sensor locations and XYZ coordinates which indicates the actual position on the bridge where sensors should be placed. Each sensor location has three DOF in X, Y, Z directions and are represented as p, q, r respectively which further aid in the identification of exact location for sensor placement.

Table 2: The ED vector with final sensor locations and coordinates for model WPT

No.	Final Sensor Location	ED	Coordinates		
			X	Y	Z
1	1873q	0.5	-1232.2	14114	0
2	1873r	0.5	-1232.2	14114	0
3	1483r	0.63707	19755	13587	0
4	1493r	0.5647	-20201	13094	0
5	1666r	0.92824	11466	14003	0
6	1027q	0.49164	-48018	10868	0
7	1027r	0.49164	-48018	10868	0
8	825r	0.49099	48576	11352	0
9	826r	0.49084	48675	11344	0
10	1661r	0.90488	-13021	13636	0

Table 3: The ED vector with final sensor locations and coordinates for model WNPT

No.	Final Sensor Location	ED	Coordinates		
			X	Y	Z
1	1492r	0.49907	19855	13580	0
2	1493r	0.50046	-20201	13094	0
3	1494r	0.49939	-20301	13086	0
4	1019q	0.97837	-47221	10933	0
5	812q	0.97601	47290	11448	0
6	1851q	0.51788	1967.7	14145	0
7	1869r	0.5	1167.7	14140	0
8	1877q	0.52775	-1632	14106	0
9	1492r	0.49907	19855	13580	0
10	1493r	0.50046	-20201	13094	0

5. The EFI-DPR Method

In the same way, ten final sensor locations are obtained but this time by multiplying the DPR with the corresponding effective independence distribution vector to ensure that locations with low energy contents are not selected.

The beam models WPT and WNPT were also used in this case and the method computed in MATLAB using similar modal parameters as those used in computation of the ED vector in the previous section. The final ED vector after the application of this method for both

bridge models with post-tension and with no post-tension case can be seen in figure 11 and 12 below. Table 4 and Table 5 also show their corresponding sensor locations with XYZ coordinates.

Table 4: The ED vector with final sensor locations and coordinates for model WNPT

No.	Final Sensor Location	ED	Coordinates		
			X	Y	Z
1	2194r	0.36524	367.72	14133	0
2	1493r	0.20795	-20201	13094	0
3	1827q	0.43971	3367.7	14148	0
4	1828q	0.43125	3267.7	14149	0
5	1019q	0.27393	-47221	10933	0
6	1020q	0.27537	-47321	10925	0
7	811q	0.27005	47191	11456	0
8	812q	0.2695	47290	11448	0
9	1859q	0.44008	-2831.8	14081	0
10	1860q	0.45363	-2931.8	14078	0
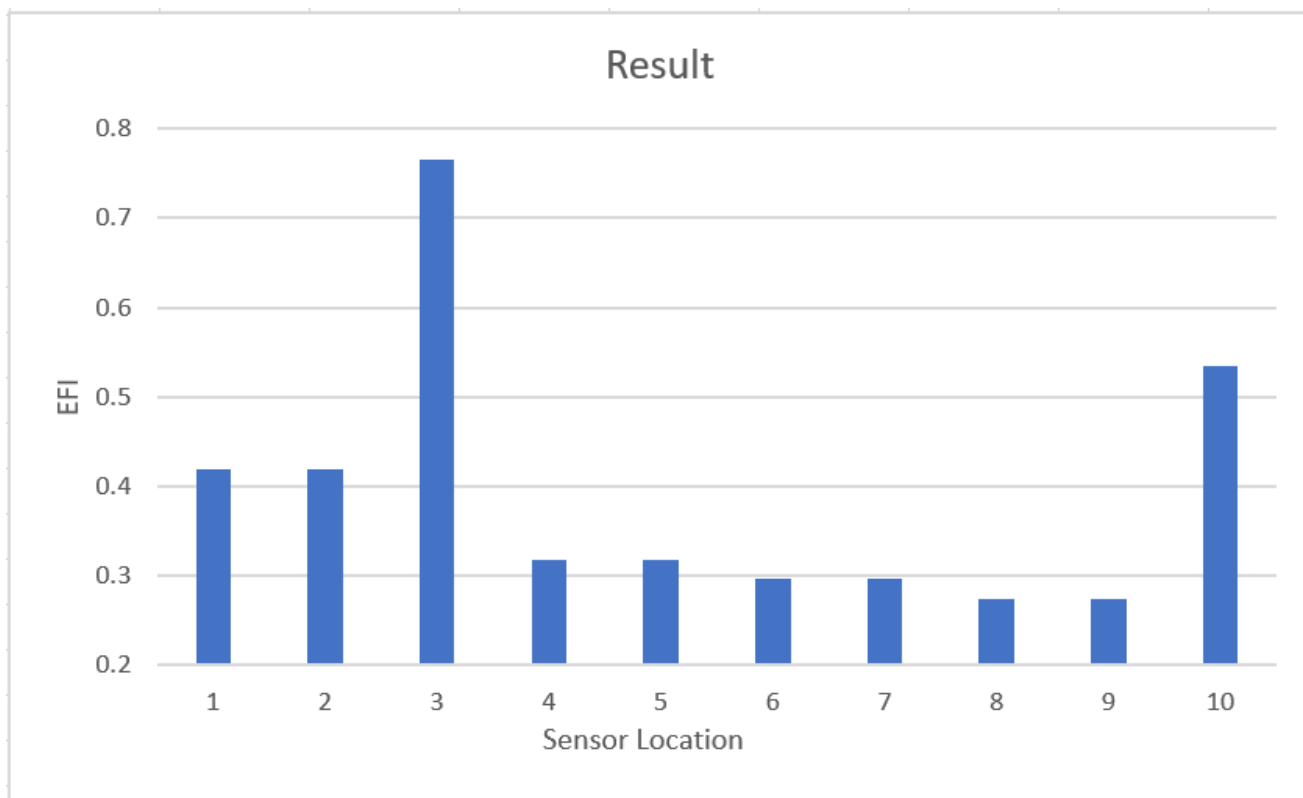
Figure 11: Bar plot of ED values for ten sensor locations for beam model with PT

Table 5: The ED vector with final sensor locations and coordinates for model WPT

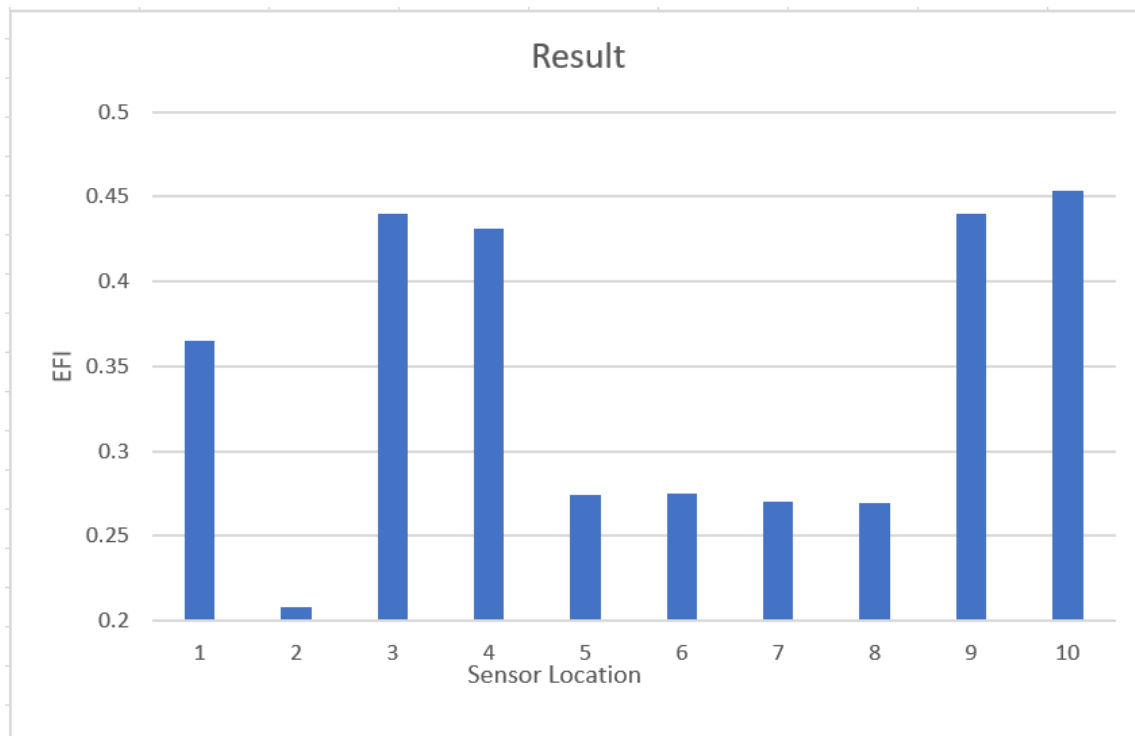| No.	Final Sensor Location	ED	Coordinates		
			X	Y	Z
1	1873q	0.41948	-1232.2	14114	0
2	1873r	0.41948	-1232.2	14114	0
3	2190r	0.7659	-1132.2	14115	0
4	1688q	0.31699	10267	14042	0
5	1688r	0.31699	10267	14042	0
6	1679q	0.2963	-11824	13710	0
7	1679r	0.2963	-11824	13710	0
8	1021q	0.27464	-47420	10917	0
9	1021r	0.27464	-47420	10917	0
10	810r	0.53455	48081	11389	0

Figure 12: Bar plot of ED values for ten sensor locations using EFI-DPR method for model WNPT

5.2. Evaluation of Methods

In the above section, the OSP methods utilized in the identification of sensor location produced different results which are seen from the final sensor locations variations obtained for each case. In order to evaluate the performance of both methods used they are compared based on the following criteria:

5.2.1. Condition Number:

The condition number (CN) is very crucial criteria for comparison of OSP methods because it determines the degree of orthogonality between mode shape vectors [9]. CN can be obtained from the singular value decomposition (SVD) of the reduced the mode shape matrix that is

$$SVD \ \Phi = \Sigma V^T U, \tag{5.0}$$

where U and V are orthogonal matrices and Σ is a diagonal matrix containing the singular values $\sigma_1, \sigma_2, \dots \sigma_N$ for N number of modes [33]. Therefore, the CN is calculated as the ratio of the largest singular value (σ_1) to the lowest singular value (σ_n) that is (see [34])

$$CN = \frac{\sigma_1}{\sigma_n} \tag{5.1}$$

If CN is close to 1, it indicates that the mode shape matrix is normally orthogonal, meaning the mode shapes are independent. A higher CN indicates a greater degree of linear dependence between the mode shapes [13].

The CN is important because it affects the accuracy of modal analysis techniques, such as modal expansion and observability. A higher CN can lead to errors in these calculations [13].

5.2.2. Determinant of the Fisher Information Matrix

The FIM as mentioned in chapter 2 evaluates the efficiency of an unbiased estimator and is derived from the minimization of the covariance matrix of the estimate error which estimates the uncertainties of parameters obtained from the dynamic test [13]. Therefore, the determinant of FIM provides an efficient index of the information acquired from the test. The larger the determinant, the more information can be obtained from the test. This means that improving the determinant of FIM can increase the amount of information gathered, which can in turn reduce the uncertainty of the estimated parameters [13].

5.2.3. Trace

The trace of the FIM is another way to determine the effectiveness of the final sensor configuration obtained from the EFI sensor placement method [9]. The trace can be obtained from the sum of the diagonal elements in the FIM.

The trace, determinant, and condition number of FIM were continuously monitored during the iteration sequence to assess the quality of the selected sensor sets during the iteration process for both EFI and the EFI-DPR. This analysis was performed and closely monitored for the first 5000 iterations on the FE model WNPT, but the resulting values for trace, determinant and condition number were recorded after every 500 iterations to save time since the total DOF for the model is 5514. After the first 1000 iterations, the sensor locations reduced to 4514 but with subsequent increment in number of iterations, the sensor locations reduced to 4014, 3514, 3014, 2514, 2014, 1514, 1014, 514 respectively.
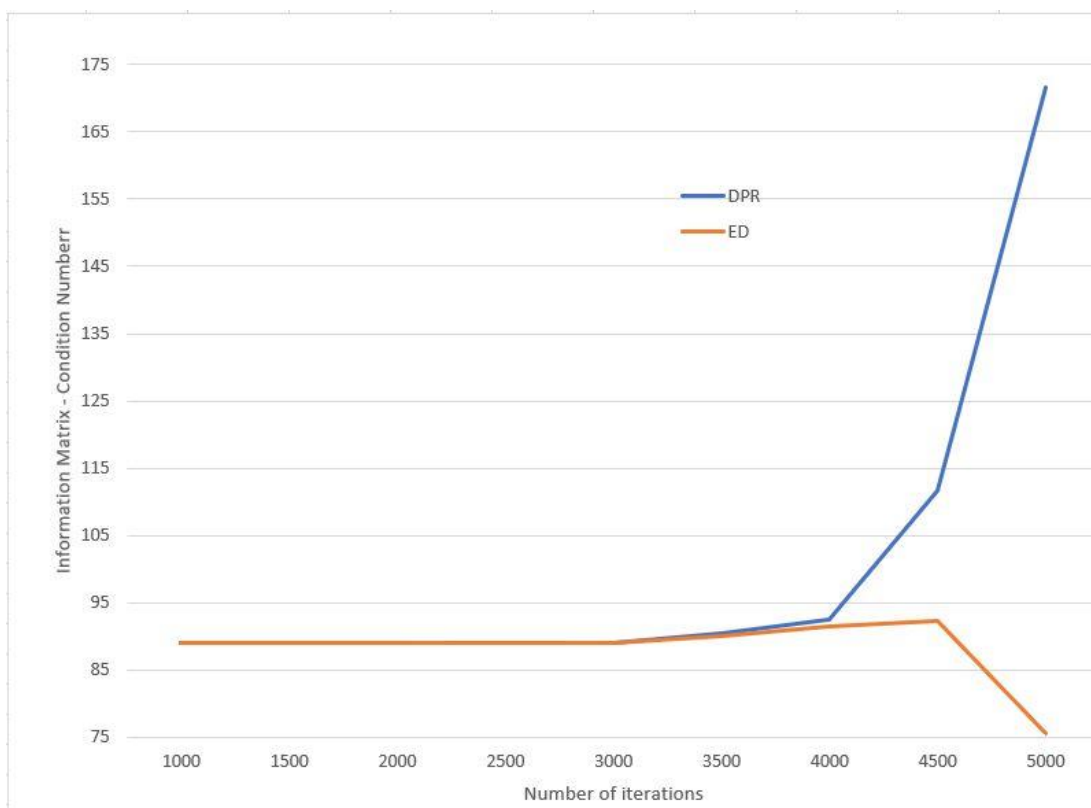
Figure 13: Condition number of Matrix A_0 vs Number of iterations

Figure 13 presents the results for the condition number of FIM. The condition numbers of the EFI based configurations and the EFI-DPR based configurations exhibit similar performance down to 2014 sensor locations, with the EFI method slightly outperforming. However, below 1514 sensor locations, the EFI-DPR proves to be even way more less efficient and the EFI method produces a sensor configuration with a significantly smaller condition number compared to the corresponding configuration based on EFI-DPR. This indicates that the estimates are less sensitive to errors in analytical modeling when using

the EFI method. Additionally, the condition number resulting from the EFI technique exhibits greater stability and predictability compared to the condition number resulting from sensor set iteration based on EFI-DPR.
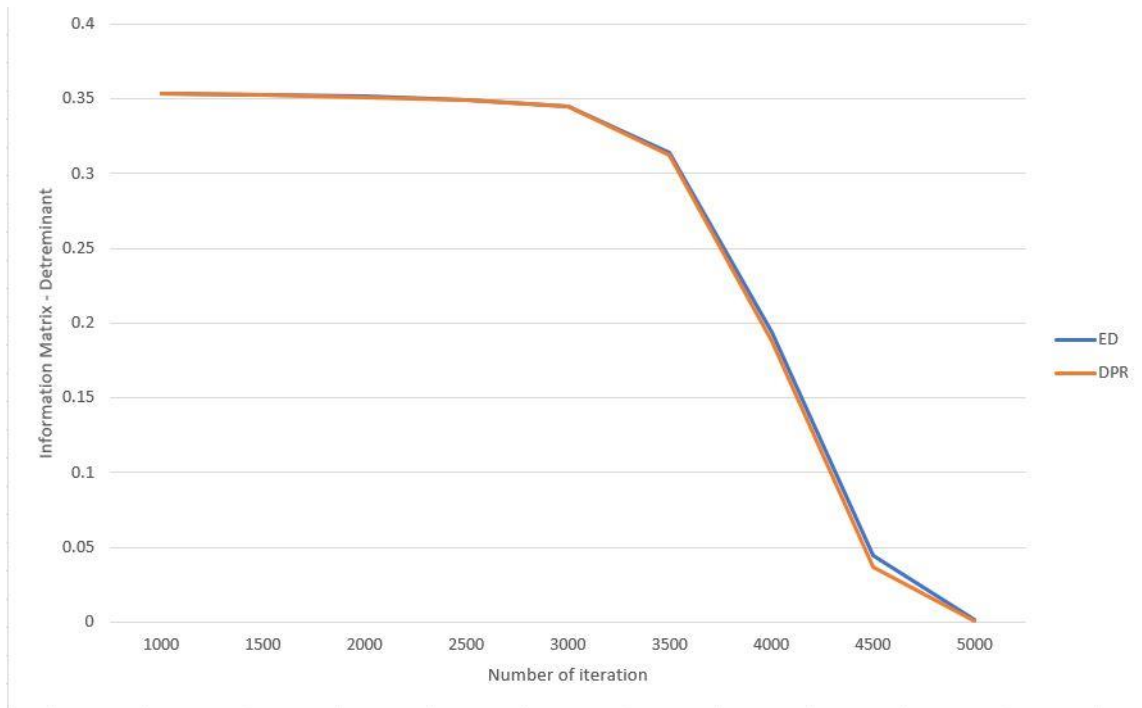
Figure 14: Determinant of matrix A_0 vs Number of iterations

The discrepancy between the EFI method and EFI-DPR is not so obvious when considering the determinant of FIM, as depicted in Figure 14. However, the sensor configurations derived from the EFI-DPR measure retain a significantly greater amount of information compared to the configurations based on EI.

Figure 15 illustrates a comparison of trace values obtained from the 5000 iterations based on both methods. The EFI-DPR method consistently yields higher trace values for the FIM compared to the EFI method. This implies that utilizing the EFI-DPR method leads to a sensor configuration with a smaller estimate error covariance matrix, resulting in improved state estimates.
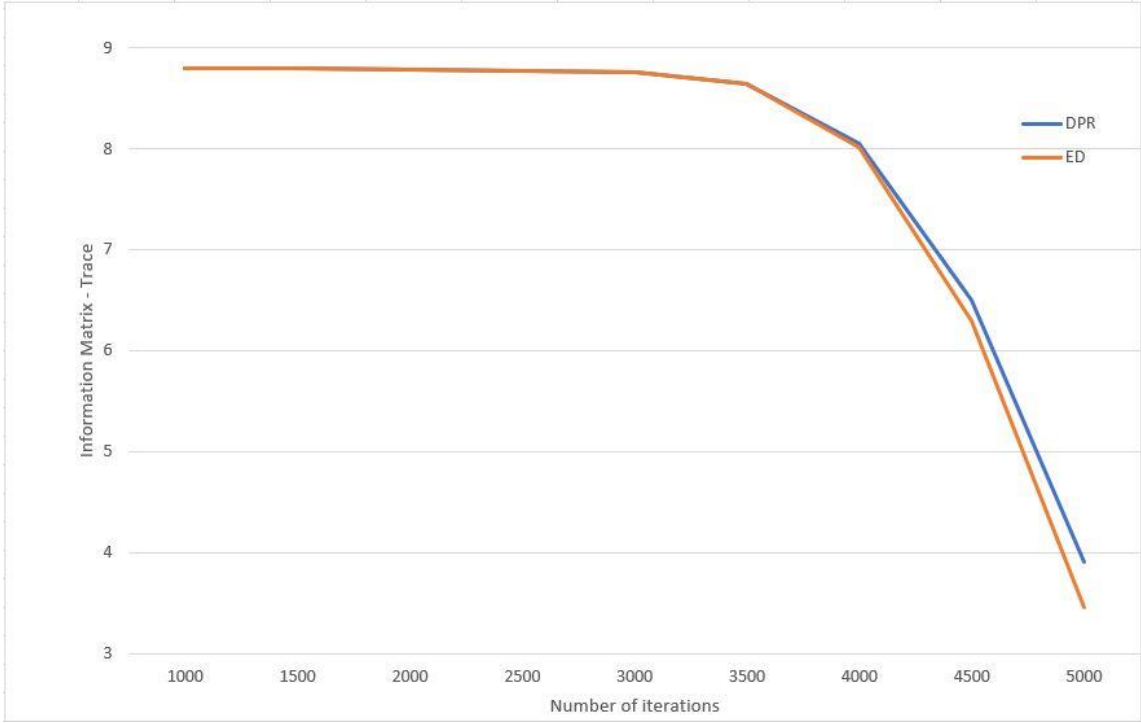
Figure 15: Trace of matrix A_0 vs Number of iterations

5. Conclusion

In this thesis, four OSP methods, namely EFI, MKE, and MinMAC are discussed, and their underlying theories and formulas are presented. Each of these methods offers a unique approach to optimal sensor placement. Different optimal sensor placement criteria utilized in the determination of suitability of sensor configuration was also discussed. The EFI method was selected for performing the optimal sensor placement on the Heroysund Bridge, and EFI-DPR method which is a modification of the former was also applied and results compared to those obtained from the EFI method.

Two different beam type FE model of the bridge are developed for this thesis. The two models are models of the bridge designed with and with no post-tensions. MATLAB code is developed to implement the OSP methods. Subsequently, both the EFI and EFI-DPR methods are executed on both model types. Both methods are iterative and ensure candidate sensor locations are reduced to a desire number. The process maximizes the determinant of the Fisher information matrix and leads to a corresponding minimization of the covariance matrix of the estimate error thereby resulting in the best estimate of the target modes. The final sensor configuration obtained from the application of these methods is evaluated to determine their effectiveness by utilizing the trace, determinant and condition number of the FIM.

Based on these analyses, the EFI-DPR method satisfied two out of the three evaluation criteria which includes the trace and determinant of the FIM proving to be a better method for maximizing the linear independence of mode shapes obtained from the model of the Heroysund Bridge

References

[1] C. R. Farrar and K. Worden, "An introduction to structural health monitoring," *Philosophical Transactions of the Royal Society A: Mathematical, Physical and Engineering Sciences*, vol. 365, no. 1851, pp. 303–315, Dec. 2006, doi: 10.1098/rsta.2006.1928.

[2] E. Mesquita, P. Antunes, F. Coelho, P. André, A. Arêde, and H. Varum, "Global overview on advances in structural health monitoring platforms," *J Civil Struct Health Monit*, vol. 6, no. 3, pp. 461–475, Jul. 2016, doi: 10.1007/s13349-016-0184-5.

[3] K. Worden and J. M. Dulieu-Barton, "An Overview of Intelligent Fault Detection in Systems and Structures," *Structural Health Monitoring*, vol. 3, no. 1, pp. 85–98, Mar. 2004, doi: 10.1177/1475921704041866.

[4] E. B. Flynn and M. D. Todd, "A Bayesian approach to optimal sensor placement for structural health monitoring with application to active sensing," *Mechanical Systems and Signal Processing*, vol. 24, no. 4, pp. 891–903, May 2010, doi: 10.1016/j.ymssp.2009.09.003.

[5] C. Scuro, P. F. Sciammarella, F. Lamonaca, R. S. Olivito, and D. L. Carni, "IoT for structural health monitoring," *IEEE Instrumentation & Measurement Magazine*, vol. 21, no. 6, pp. 4–14, Dec. 2018, doi: 10.1109/MIM.2018.8573586.

[6] H.-N. Li, L. Ren, Z.-G. Jia, T.-H. Yi, and D.-S. Li, "State-of-the-art in structural health monitoring of large and complex civil infrastructures," *J Civil Struct Health Monit*, vol. 6, no. 1, pp. 3–16, Feb. 2016, doi: 10.1007/s13349-015-0108-9.

[7] F. Lamonaca, P. F. Sciammarella, C. Scuro, D. L. Carnì, and R. S. Olivito, "Internet of Things for Structural Health Monitoring," in *2018 Workshop on Metrology for Industry 4.0 and IoT*, Apr. 2018, pp. 95–100. doi: 10.1109/METROI4.2018.8439038.

[8] F. E. Udwadia, "Methodology for optimum sensor locations for parameter identitfication in dynamic systems," *Journal of Engineering Mechanics*, vol. 120, no. 2, pp. 368–390, 1994.

[9] D. C. Kammer, "Sensor placement for on-orbit modal identification and correlation of large space structures," *Journal of Guidance, Control, and Dynamics*, vol. 14, no. 2, pp. 251–259, Mar. 1991, doi: 10.2514/3.20635.

[10] D. C. Kammer, "Effects of Noise on Sensor Placement for On-Orbit Modal Identification of Large Space Structures," *Journal of Dynamic Systems, Measurement, and Control*, vol. 114(3), pp. 436–442, Sep. 1992, doi: https://doi.org/10.1115/1.2897366.

[11] F. Sunca, F. Y. Okur, A. C. Altunişik, and V. Kahya, "Optimal Sensor Placement for Laminated Composite and Steel Cantilever Beams by the Effective Independence Method," *Structural Engineering International*, vol. 31, no. 1, pp. 85–92, Jan. 2021, doi: 10.1080/10168664.2019.1704202.

[12] M. I. Friswell and R. Castro-Triguero, "Clustering of Sensor Locations Using the Effective Independence Method," *AIAA Journal*, vol. 53, no. 5, pp. 1388–1391, 2015, doi: 10.2514/1.J053503.

[13] B. Li, J. Ou, X. Zhao, and D. Li, *Optimal Sensor placement in Health Monitoring System of Xinghai Bay Bridge*. 2011.

[14] M. Meo and G. Zumpano, "On the optimal sensor placement techniques for a bridge structure," *Engineering Structures*, vol. 27, no. 10, pp. 1488–1497, Aug. 2005, doi: 10.1016/j.engstruct.2005.03.015.

[15] C. Leyder, V. Dertimanis, A. Frangi, E. Chatzi, and G. Lombaert, "Optimal sensor placement methods and metrics – comparison and implementation on a timber frame structure," *Structure and Infrastructure Engineering*, vol. 14, no. 7, pp. 997–1010, Jul. 2018, doi: 10.1080/15732479.2018.1438483.

[16] T. G. Carne and C. R. Dohrmann, "A modal test design strategy for model correlation," Sandia National Labs., Albuquerque, NM (United States), SAND-94-2702C; CONF-950240-4, Dec. 1994. Accessed: Apr. 21, 2023. [Online]. Available: https://www.osti.gov/biblio/10103444

[17] B. Li, D. Li, X. Zhao, and J. Ou, "Optimal sensor placement in health monitoring of suspension bridge," *Sci. China Technol. Sci.*, vol. 55, no. 7, pp. 2039–2047, Jul. 2012, doi: 10.1007/s11431-012-4815-8.

[18] M. Lizana and J. R. Casas, "Robustness of Optimal Sensor Methods in Dynamic Testing–Comparison and Implementation on a Footbridge," *Dynamics*, vol. 2, no. 2, Art. no. 2, Jun. 2022, doi: 10.3390/dynamics2020007.

[19] C. Papadimitriou, J. L. Beck, and S.-K. Au, "Entropy-Based Optimal Sensor Location for Structural Model Updating," *Journal of Vibration and Control*, vol. 6, no. 5, pp. 781–800, Jul. 2000, doi: 10.1177/107754630000600508.

[20] J. Zhang, K. Maes, G. De Roeck, E. Reynders, C. Papadimitriou, and G. Lombaert, "Optimal sensor placement for multi-setup modal analysis of structures," *Journal of Sound and Vibration*, vol. 401, pp. 214–232, Aug. 2017, doi: 10.1016/j.jsv.2017.04.041.

[21] D. S. Li, H. N. Li, and C. P. Fritzen, "The connection between effective independence and modal kinetic energy methods for sensor placement," *Journal of Sound and Vibration*, vol. 305, no. 4, pp. 945–955, Sep. 2007, doi: 10.1016/j.jsv.2007.05.004.

[22] T.-H. Yi and H.-N. Li, "Methodology Developments in Sensor Placement for Health Monitoring of Civil Infrastructures," *International Journal of Distributed Sensor Networks*, vol. 8, no. 8, p. 612726, Aug. 2012, doi: 10.1155/2012/612726.

[23] M. Pastor, M. Binda, and T. Harčarik, "Modal Assurance Criterion," *Procedia Engineering*, vol. 48, pp. 543–548, Jan. 2012, doi: 10.1016/j.proeng.2012.09.551.

[24] M. Lizana and J. R. Casas, "Optimal sensor placement methods and criteria in dynamic testing - comparison and implementation on a pedestrian bridge".

[25] F. E. Udwadia and J. Garba, "Optimal Sensor Locations for Structural Identification," Apr. 1985. Accessed: Mar. 04, 2023. [Online]. Available: https://ntrs.nasa.gov/citations/19850022896

[26] F. C. Schweppe, *Estimation: Static linear systems. In Uncertain Dynamic Systems*. Prentice Hall, 1973.

[27] G. Heo, M. L. Wang, and D. Satpathi, "Optimal transducer placement for health monitoring of long span bridge," *Soil Dynamics and Earthquake Engineering*, vol. 16, no. 7–8, pp. 495–502, Jan. 1997, doi: 10.1016/S0267-7261(97)00010-9.

[28] N. Imamovic, "Model validation of large finite element model using test data," Imperial College London, Ph.D. dissertation, 1998.

[29] J. Guyan R., "Reduction of stiffness and mass matrices.," *AIAA Journal*, vol. 3, no. 2, p. 380, 1965, doi: 10.2514/3.2874.

[30] A. Sveen, "18-1069 Herøysund bru. Bæreevneberegninger".

[31] R. Antonsen, A. Karlsson, and B. Täljsten, "Mats Holmqvist (DEKRA Industrial AB)".

[32] P. Norheim Berg, "Beam based finite element modelling of Herøysund bridge," Norway, Masters thesis, May 2023.

[33] K. Lange, "Singular Value Decomposition," in *Numerical Analysis for Statisticians*, K. Lange, Ed., in Statistics and Computing. New York, NY: Springer, 2010, pp. 129–142. doi: 10.1007/978-1-4419-5945-4_9.

[34] W. Ostachowicz, R. Soman, and P. Malinowski, "Optimization of sensor placement for structural health monitoring: a review," *Structural Health Monitoring*, vol. 18, no. 3, pp. 963–988, May 2019, doi: 10.1177/1475921719825601.

Appendices

Appendix A

Appendix A contains MATLAB plots of the result from both EFI and ERFI-DPR methods applied on the bridge model.
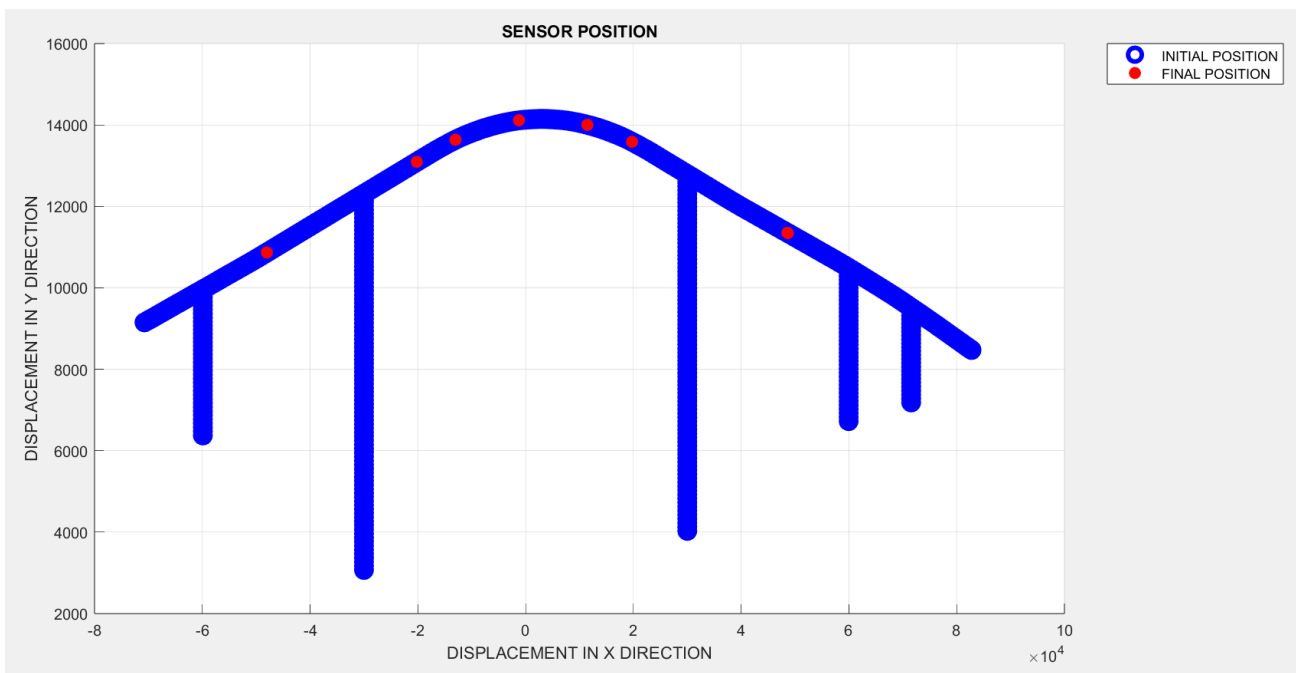

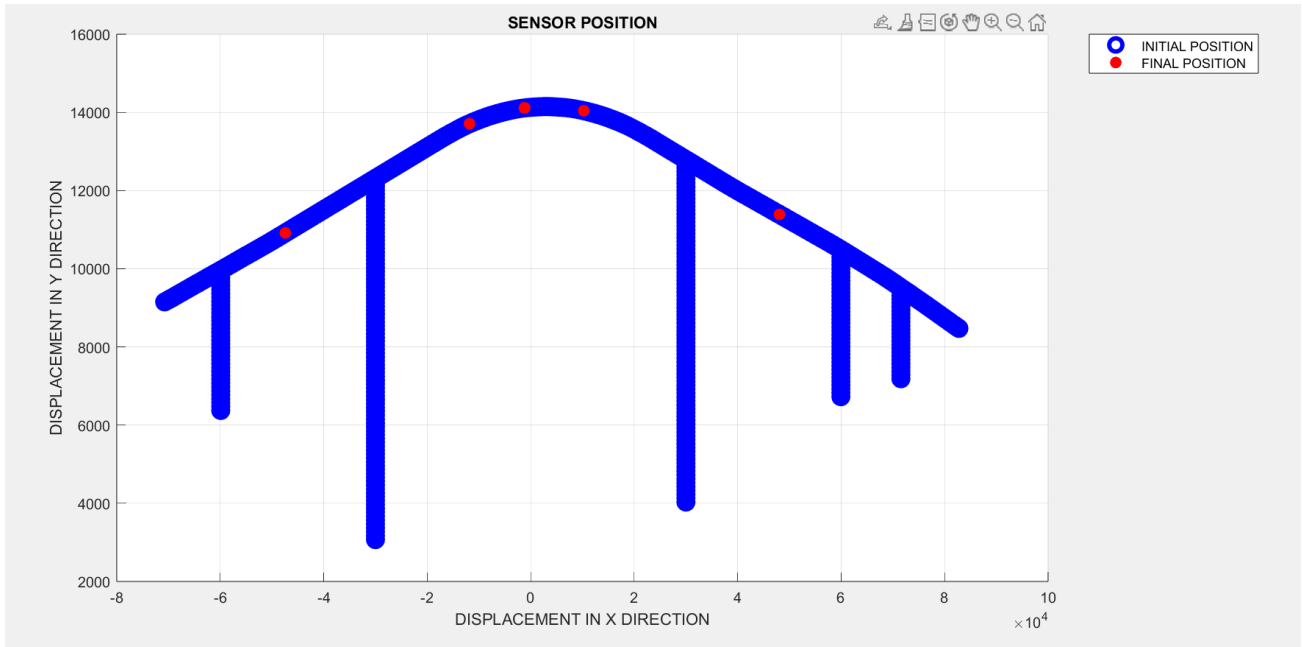Figure A-1 1: ten final sensor locations for model WPT

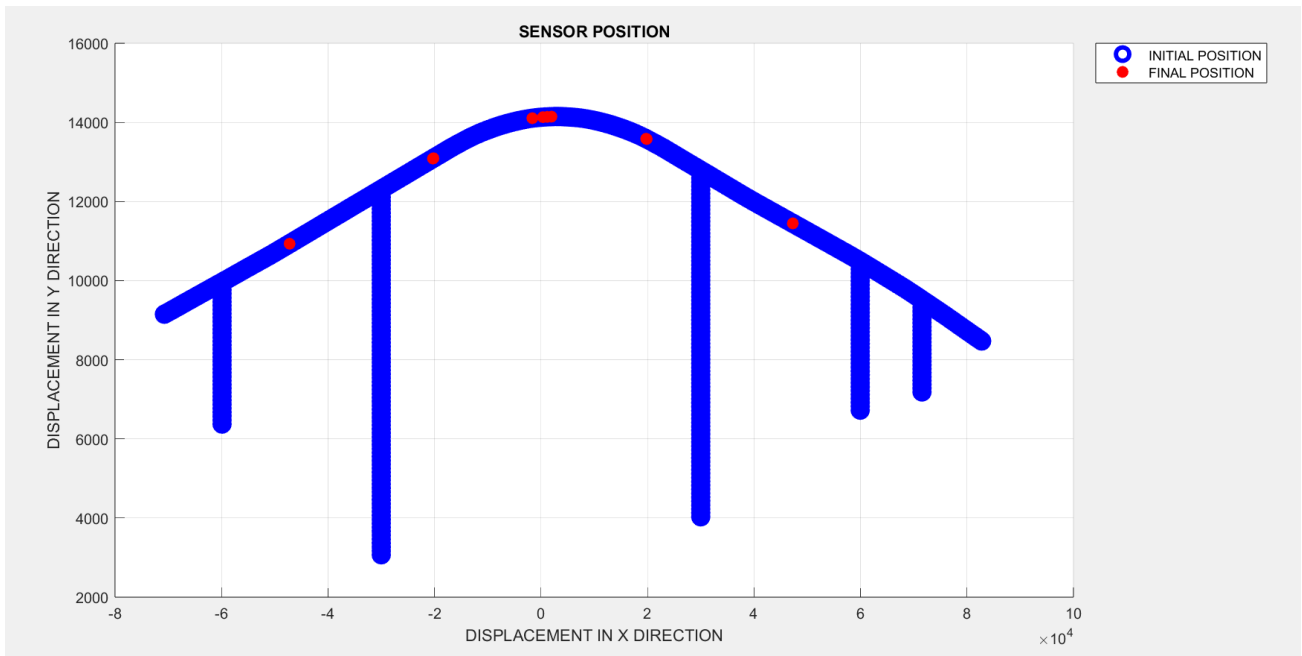Figure A-1 2: Ten sensor locations for model WPT EFI-DPR method

Figure A-1 3: Ten final sensor location for model WNPT
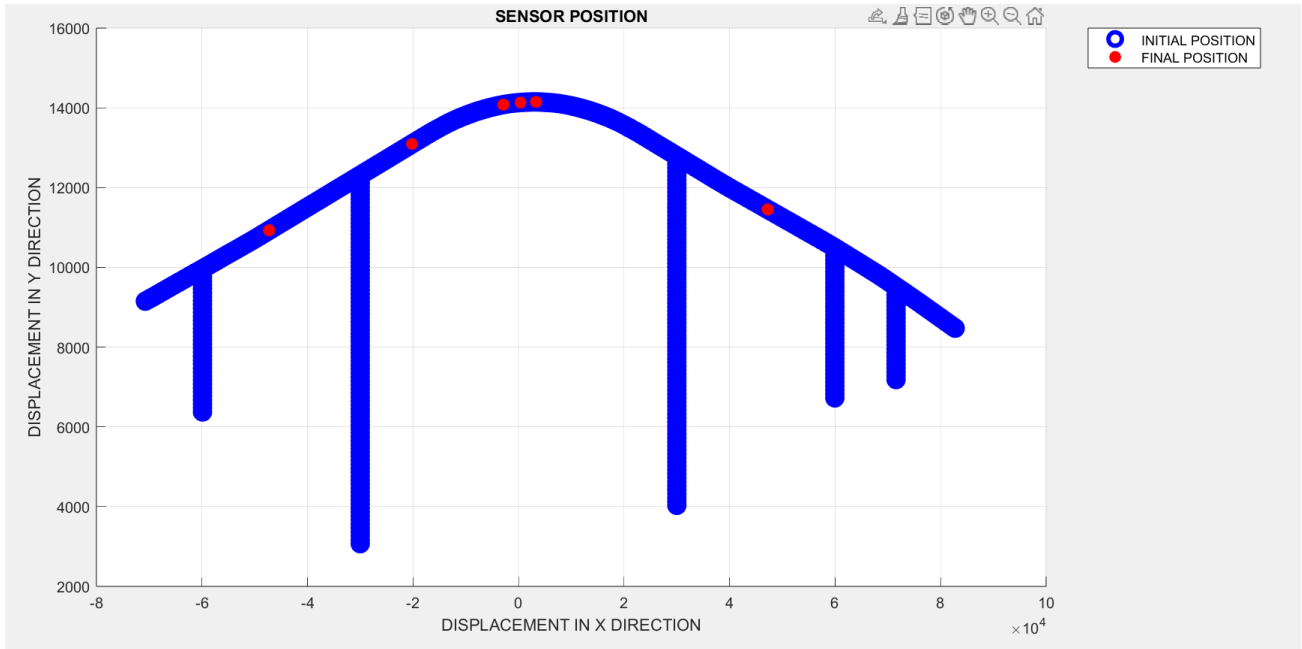
Figure A-1 4: Ten sensor location for model WNPT EFI-DPR method

Appendix B

Appendix B contains the 20 mode shapes and their frequencies for bridge model.

Table A-1: Beam model with no post tensioning

Mode	Frequency [Hz]	Mode	Frequency [Hz]
1	1.4407	1.	1.4413
2.	2.2387	2.	2.2388
3.	2.3951	3.	2.3961
4.	2.9588	4.	2.9593
5.	3.5732	5.	3.574
6.	4.1455	6.	4.1456
7.	4.8339	7.	4.8346
8.	5.1074	8.	5.1084
9.	5.1398	9.	5.1408
10.	5.1825	10.	5.1836
11.	5.3577	11.	5.3579
12.	7.1458	12.	7.1466
13.	7.3409	13.	7.342
14.	7.489	14.	7.4897
15.	8.8081	15.	8.8081
16.	9.6121	16.	9.6139
17.	9.9351	17.	9.9369
18.	10.022	18.	10.023
19.	10.183	19.	10.185
20.	11.182	20.	11.183

Appendix C

Appendix c contains the MATLAB code for the EFI method.

```matlab
clc
clear %to clear variables from the workspace

%importP is the  matrix with x,y,z position vectors and total displacement

importP=readmatrix("XYZ.xlsx");% import all the mode shapes obtained from modal
analysis. total import must correspond with value of q

importP(:,1)=[];
importP(:,4)=[];

co_odMat=importP; % the  nodal coordinate or position matrix

Coox=co_odMat(:,1);
Cooy=co_odMat(:,2);
Cooz=co_odMat(:,3);

plot_position=plot3(Coox,Cooy,Cooz,'bo',LineWidth=3,MarkerSize=10);


% DISPLACEMENT FOR FIRST MODESHAPE

import1=readmatrix("DEFX1.xlsx");
import2=readmatrix("DEFY1.xlsx");
import3=readmatrix("DEFZ1.xlsx");

DEF1=[import1,import2,import3];   % X,Y,Z DISPLACEMENT MATRIX FOR MODE 1

Pos=DEF1(:,1); % total number of nodes or rows in the matrix

DEF1_D=DEF1(:,[5,10,15]);

% rearrange matrix
DEF1_R = reshape(DEF1_D', [], 1);


% DISPLACEMENT FOR SECOND MODESHAPE

import4=readmatrix("DEFX2.xlsx");
```

```matlab
import5=readmatrix("DEFY2.xlsx");
import6=readmatrix("DEFZ2.xlsx");

DEF2=[import4,import5,import6];   % X,Y,Z DISPLACEMENT MATRIX FOR MODE 2
DEF2_D=DEF2(:,[5,10,15]);

% rearrange matrix
DEF2_R = reshape(DEF2_D', [], 1);

% DISPLACEMENT FOR THIRD MODESHAPE

import7=readmatrix("DEFX3.xlsx");
import8=readmatrix("DEFY3.xlsx");
import9=readmatrix("DEFZ3.xlsx");
DEF3=[import7,import8,import9];   % X,Y,Z DISPLACEMENT MATRIX FOR MODE 3

DEF3_D=DEF3(:,[5,10,15]);

% rearrange matrix
DEF3_R = reshape(DEF3_D', [], 1);



% DISPLACEMENT FOR FOURTH MODESHAPE

import10=readmatrix("DEFX4.xlsx");
import11=readmatrix("DEFY4.xlsx");
import12=readmatrix("DEFZ4.xlsx");

DEF4=[import10,import11,import12];   % X,Y,Z DISPLACEMENT MATRIX FOR MODE 6
DEF4_D=DEF4(:,[5,10,15]);

% rearrange matrix
DEF4_R = reshape(DEF4_D', [], 1);



% DISPLACEMENT FOR FIFTH MODESHAPE

import13=readmatrix("DEFX5.xlsx");
import14=readmatrix("DEFY5.xlsx");
import15=readmatrix("DEFZ5.xlsx");

DEF5=[import13,import14,import15];   % X,Y,Z DISPLACEMENT MATRIX FOR MODE 6
DEF5_D=DEF5(:,[5,10,15]);
```

```matlab
% rearrange matrix
DEF5_R = reshape(DEF5_D', [], 1);


% DISPLACEMENT FOR SIXTH MODESHAPE

import16=readmatrix("DEFX6.xlsx");
import17=readmatrix("DEFY6.xlsx");
import18=readmatrix("DEFZ6.xlsx");

DEF6=[import16,import17,import18];   % X,Y,Z DISPLACEMENT MATRIX FOR MODE 6
DEF6_D=DEF6(:,[5,10,15]);

% rearrange matrix
DEF6_R = reshape(DEF6_D', [], 1);

% Full matrix containing all mode shapes and candidate sensorlocations in x,y,z directions
Main_Mat=[DEF1_R,DEF2_R,DEF3_R, DEF4_R,DEF5_R,DEF6_R];


m=6; % Target modes
n=10; % Total number of sensor to be installed/final number of sensor
q=6; % total number of mode shapes obtained from modal analysis

    M_Mat=Main_Mat;

z=size(M_Mat);
y=z(1,1);


s=size(Pos);
o=s(1,1);

j=3; % change the number here depending on the number of DOF considered
if j==1 % % node + number of DOF in this case 1 DOFs
    for t=1:o
        A=[Pos(t,1)+"z"]; % change the direction depending on the direction being studied
        if t==1
            POS=A;
        end
        if t>1
            POS=[POS;A];
        end
    end
end
```

```matlab
if j==2 % node + number of DOF in this case 2 DOFs
    for t=1:o
        A=[Pos(t,1)+"x";Pos(t,1)+"y"];
        if t==1
            POS=A;
        end
        if t>1
            POS=[POS;A];
        end
    end
end

if j==3 % node + number of DOF in this case 3 DOFs
    for t=1:o
        A=[Pos(t,1)+"x";Pos(t,1)+"y";Pos(t,1)+"z"];
        if t==1
            POS=A;
        end
        if t>1
            POS=[POS;A];
        end
    end
end


if j==1 % node + number of DOF in this case 3 DOFs  j=1
    COO=co_odMat;
End

if j==2 % node + number of DOF in this case 3 DOFs  j=2

    for t=1:o
        B=[co_odMat(t,:);co_odMat(t,:)];
        if t==1
            COO=B;
        end
        if t>1
            COO=[COO;B];
        end
    end
end
if j==3 % node + number of DOF in this case 3 DOFs  j=3
    for t=1:o
        B=[co_odMat(t,:);co_odMat(t,:);co_odMat(t,:)];
        if t==1
            COO=B;
```

```matlab
        end
        if t>1
            COO=[COO;B];
        end
    end
  end
end



for t=1:(y-n) %number of cycles
    v=size(M_Mat);
    g=v(1,1);
    h=v(1,2);

    % EID method
    for k=1:g
        D=M_Mat(k,:)'*M_Mat(k,:); %Fisher Information Matrix
        if k==1
            FM=D;
        end
        if k>1
            FM=FM+D; % FIM
        end
    end

    [VE,VA]=eig(FM); %Pcalculate eigenvale and eigen vector

    G=(M_Mat*VE).*(M_Mat*VE); %obtain G matrix using term by term product

    VAI=inv(VA); %obtain the inverse of matrix

    Fe=G*VAI; %calculate FE matrix

    Ed=sum(Fe')'; %ED vector

    [Val_Min,Row_Min]=min(Ed); %the minimum Ed vector

    M_Mat(Row_Min,:)=[]; %delete row coresponding to the minimum Ed value from mode
shape matrix

    POS(Row_Min,:)=[]; %delete corresponding row in the DOF column vector

    COO(Row_Min,:)=[]; %delete row of the coresonding coordinate matrix
end

v=size(M_Mat);
```

```matlab
    g=v(1,1);
    h=v(1,2);
    for k=1:g
       D=M_Mat(k,:)'*M_Mat(k,:);
       if k==1
          FM=D;
       End

       if k>1
          FM=FM+D;
       end
    end

    [VE,VA]=eig(FM);
    G=(M_Mat*VE).*(M_Mat*VE);
    VAI=inv(VA);
    Fe=G*VAI;
    Ed=sum(Fe')';

RESULT=[POS Ed COO];


Coox=co_odMat(:,1);
Cooy=co_odMat(:,2);
Cooz=co_odMat(:,3);

COOx=COO(:,1);
COOy=COO(:,2);
COOz=COO(:,3);

graficostart=plot3(Coox,Cooy,Cooz,'bo',LineWidth=3,MarkerSize=10);

hold on % adds the two graphs to give initial and final locations

graficofinish=plot3(COOx,COOy,COOz,'ro',LineWidth=5,MarkerSize=3);


xlabel('DISPLACEMENT IN X DIRECTION');
ylabel('DISPLACEMENT IN Y DIRECTION');
zlabel('DISPLACEMENT IN Z DIRECTION');
title('SENSOR POSITION');
grid on;
legend('INITIAL POSITION','FINAL POSITION');
```

Appendix D

Appendix D contains the MATLAB code for the EFI-DPR method.

```
clc
clear %to clear variables from the workspace

importF=readmatrix("MODESHAPES.xlsx");

importF(:,1:2)=[];
importF(1,:)=[];
importF(7:20,:)=[];
fre_q=importF;
fre_w=2*pi*fre_q;
inv_fre_w=1./fre_w;

%importP is the  matrix with x,y,z position vectors and total displacement

importP=readmatrix("XYZ.xlsx");% import all the mode shapes obtained from modal
analysis. total import must correspond with value of q

importP(:,1)=[];
importP(:,4)=[];

co_odMat=importP; % the  nodal coordinate or position matrix

Coox=co_odMat(:,1);
Cooy=co_odMat(:,2);
Cooz=co_odMat(:,3);

plot_position=plot3(Coox,Cooy,Cooz,'bo',LineWidth=3,MarkerSize=10);


% DISPLACEMENT FOR FIRST MODESHAPE

import1=readmatrix("DEFX1.xlsx");
import2=readmatrix("DEFY1.xlsx");
import3=readmatrix("DEFZ1.xlsx");

DEF1=[import1,import2,import3];   % X,Y,Z DISPLACEMENT MATRIX FOR MODE 1
Pos=DEF1(:,1); % total number of nodes or rows in the matrix
DEF1_D=DEF1(:,[5,10,15]);

% rearrange matrix
```

```matlab
DEF1_R = reshape(DEF1_D', [], 1);


% DISPLACEMENT FOR SECOND MODESHAPE

import4=readmatrix("DEFX2.xlsx");
import5=readmatrix("DEFY2.xlsx");
import6=readmatrix("DEFZ2.xlsx");

DEF2=[import4,import5,import6];   % X,Y,Z DISPLACEMENT MATRIX FOR MODE 2
DEF2_D=DEF2(:,[5,10,15]);

% rearrange matrix
DEF2_R = reshape(DEF2_D', [], 1);

% DISPLACEMENT FOR THIRD MODESHAPE

import7=readmatrix("DEFX3.xlsx");
import8=readmatrix("DEFY3.xlsx");
import9=readmatrix("DEFZ3.xlsx");

DEF3=[import7,import8,import9];   % X,Y,Z DISPLACEMENT MATRIX FOR MODE 3
DEF3_D=DEF3(:,[5,10,15]);

% rearrange matrix
DEF3_R = reshape(DEF3_D', [], 1);



% DISPLACEMENT FOR FOURTH MODESHAPE

import10=readmatrix("DEFX4.xlsx");
import11=readmatrix("DEFY4.xlsx");
import12=readmatrix("DEFZ4.xlsx");

DEF4=[import10,import11,import12];   % X,Y,Z DISPLACEMENT MATRIX FOR MODE 6
DEF4_D=DEF4(:,[5,10,15]);

% rearrange matrix
DEF4_R = reshape(DEF4_D', [], 1);


% DISPLACEMENT FOR FIFTH MODESHAPE

import13=readmatrix("DEFX5.xlsx");
import14=readmatrix("DEFY5.xlsx");
```

```matlab
import15=readmatrix("DEFZ5.xlsx");

DEF5=[import13,import14,import15];   % X,Y,Z DISPLACEMENT MATRIX FOR MODE 6
DEF5_D=DEF5(:,[5,10,15]);

% rearrange matrix
DEF5_R = reshape(DEF5_D', [], 1);

% DISPLACEMENT FOR SIXTH MODESHAPE

import16=readmatrix("DEFX6.xlsx");
import17=readmatrix("DEFY6.xlsx");
import18=readmatrix("DEFZ6.xlsx");

DEF6=[import16,import17,import18];   % X,Y,Z DISPLACEMENT MATRIX FOR MODE 6
DEF6_D=DEF6(:,[5,10,15]);

% rearrange matrix
DEF6_R = reshape(DEF6_D', [], 1);

% Full matrix containing all mode shapes and candidate sensorlocations in x,y,z directions

Main_Mat=[DEF1_R,DEF2_R,DEF3_R, DEF4_R,DEF5_R,DEF6_R];

m=6; % Target modes
n=10; % Total number of sensor to be installed/final number of sensors
q=6; % total number of mode shapes obtained from modal analysis


    M_Mat=Main_Mat;


z=size(M_Mat);
y=z(1,1);


s=size(Pos);
o=s(1,1);

j=3; % change the number here depending on the number of DOF considered
if j==1 % % node + number of DOF in this case 1 DOFs
    for t=1:o
        A=[Pos(t,1)+"z"]; % change the direction depending on the direction being studied
        if t==1
            POS=A;
        end
        if t>1
```

```matlab
                POS=[POS;A];
            end
        end
    end
    if j==2 % node + number of DOF in this case 2 DOFs
        for t=1:o
            A=[Pos(t,1)+"x";Pos(t,1)+"y"];
            if t==1
                POS=A;
            end
            if t>1
                POS=[POS;A];
            end
        end
    end
    if j==3 % node + number of DOF in this case 3 DOFs
        for t=1:o
            A=[Pos(t,1)+"x";Pos(t,1)+"y";Pos(t,1)+"z"];
            if t==1
                POS=A;
            end
            if t>1
                POS=[POS;A];
            end
        end
    end


    if j==1 % node + number of DOF in this case 3 DOFs  j=1
        COO=co_odMat;
    end
    if j==2 % node + number of DOF in this case 3 DOFs  j=2
        for t=1:o
            B=[co_odMat(t,:);co_odMat(t,:)];
            if t==1            COO=B;
            end
            if t>1
                COO=[COO;B];
            end
        end
    end
    if j==3 % node + number of DOF in this case 3 DOFs  j=3
        for t=1:o
            B=[co_odMat(t,:);co_odMat(t,:);co_odMat(t,:)];
            if t==1
                COO=B;
```

```matlab
        end
        if t>1
            COO=[COO;B];
        end
    end
end

 for t=1:(y-n) %number of cycles
    v=size(M_Mat);
    g=v(1,1);
    h=v(1,2);


DPR=zeros(g,1);

for i=1:g
    for j=1:h
      DPR(i)=DPR(i)+ M_Mat(i,j)^2 /fre_w(j);
     end
end


    % EID method
    for k=1:g
        D=M_Mat(k,:)'*M_Mat(k,:); %Fisher Information Matrix
        if k==1
            FM=D;
        end
        if k>1
            FM=FM+D; % FIM
        end
    end
    [VE,VA]=eig(FM); %Pcalculate eigenvale and eigen vector
    G=(M_Mat*VE).*(M_Mat*VE); %obtain G matrix using term by term product
    VAI=inv(VA); %obtain the inverse of matrix
    Fe=G*VAI; %calculate FE matrix
    Ed=sum(Fe')'; %ED vector
    Ed_new=Ed.*DPR;%new ED vector weighted by DPR
    [Val_Min,Row_Min]=min(Ed_new); %the minimum Ed vector
    M_Mat(Row_Min,:)=[]; %delete row coresponding to the minimum Ed value from mode
shape matrix
    POS(Row_Min,:)=[]; %delete corresponding row in the DOF column vector
COO(Row_Min,:)=[]; %delete row of the coresonding coordinate matrix
    Ed_new(Row_Min,:)=[]; %delete row of the coresonding coordinate matrix
    DPR(Row_Min,:)=[]; %delete row of the coresonding coordinate matrix
end
```

```matlab
v=size(M_Mat);
   g=v(1,1);
   h=v(1,2);
   for k=1:g
      D=M_Mat(k,:)'*M_Mat(k,:);
      if k==1
         FM=D;
      end
      if k>1
         FM=FM+D;
      end
   end
   [VE,VA]=eig(FM);
   G=(M_Mat*VE).*(M_Mat*VE);
   VAI=inv(VA);
   Fe=G*VAI;
   Ed=sum(Fe')'; %ED vector
   Ed_new=Ed.*DPR;

RESULT=[POS Ed_new COO];


Coox=co_odMat(:,1);
Cooy=co_odMat(:,2);
Cooz=co_odMat(:,3);
COOx=COO(:,1);
COOy=COO(:,2);
COOz=COO(:,3);

graficostart=plot3(Coox,Cooy,Cooz,'bo',LineWidth=3,MarkerSize=10);
hold on % adds the two graphs to output plot showing initial and final sensor locations
graficofinish=plot3(COOx,COOy,COOz,'ro',LineWidth=5,MarkerSize=3);



xlabel('DISPLACEMENT IN X DIRECTION');
ylabel('DISPLACEMENT IN Y DIRECTION');
zlabel('DISPLACEMENT IN Z DIRECTION');
title('SENSOR POSITION');
grid on;
legend('INITIAL POSITION','FINAL POSITION');
```

Appendix E

Site visit

The structural health of structures is very crucial and just like the health of humans it should be monitored and maintained to promote longevity. Doctors play an important role in improving the well-being of humans but for structures sensors are deployed. My thesis topic is focused on optimal placement of sensors on the Herøysund Bridge in Herøy. The bridge which was built in 1960s has been exposed to various weather and loading conditions which has led to its current state of complete deterioration

I was delighted to go on a two- day visit to Heroysund Bridge with my classmate Zeeshan Azad and my thesis supervisor Dr. Harpal Singh. I consider this a valuable experience because I got the opportunity to interact with a structure that I been studying and the platform to meet with experts and an inspiring team at Nordland fylkeskommune who are committed to maintenance and development of infrastructure in Norway.

The meetings and site visitations helped develop a better connection with this thesis project. I was able to fully understand from a different perspective its significance and the great impact information obtained from this research work would have especially when applied to similar structures or bridges across Norway. The biggest highlight of my trip was connecting with some of the people working on this project especially Per Ove Ravatsås, one of the managers of this project, who presented some ongoing and future projects to us. He also shared some of his personal experiences that left me even more inspired. I am so excited to be part of a project this important and look forward to its impact on similar structures in the country.